

Multiscale modeling of transient problems in periodic Cauchy materials: asymptotic and spectro-hierarchical homogenization

Alessandro Fortunati¹, Francesca Fantoni^{2,*}, Andrea Bacigalupo¹

¹ DICCA, Università degli Studi di Genova, Genoa, Italy

² DICATAM, Università degli Studi di Brescia, Brescia, Italy

February 20, 2026

Abstract

This work presents a detailed and systematic analytical investigation of the transient elastic wave propagation in two-dimensional periodic heterogeneous composites. The study is conducted through two complementary methodologies: asymptotic homogenization and a newly proposed spectro-hierarchical approach, specifically designed to resolve higher-order microstructural effects. The asymptotic homogenization method derives effective macroscopic equations that accurately capture the averaged behavior of the periodic microstructure, providing a reduced-order but reliable representation of long-wave and low-frequency dynamics. In parallel, the spectro-hierarchical approach systematically reconstructs microstructural fluctuations using a combination of truncated Fourier expansions and a hierarchical sequence of differential problems, allowing the recovery of both first-order homogenized responses and higher-order corrections due to local heterogeneities. The analysis considers both zero and non-zero initial conditions, enabling the study of general transient excitations, including short-time dynamics and localized disturbances, rather than merely steady-state or frequency-limited responses.

1 Introduction

The rapid evolution of advanced additive manufacturing and 3D printing technologies has enabled the design and realization of architected materials and metamaterials with complex, periodic microstructures that were previously unattainable [1–5]. As a result, the development of accurate and efficient multiscale modeling strategies has become essential in order to truthfully predict the response of such materials [6, 7]. Homogenization and multiscale approaches constitute indispensable tools for capturing the macroscale behavior emerging from the microstructural architecture, offering a computationally tractable alternative to the direct simulation of fully heterogeneous systems. In this perspective, the present paper aims to compare the asymptotic homogenization scheme with the spectro-hierarchical approach proposed in [?], focusing attention on the analysis of transient elastic wave propagation in microstructured composite materials. The asymptotic homogenization technique is known to be a powerful multiscale method that accurately describes the behavior of heterogeneous microstructured materials, capturing how phenomena occurring at the microscale influence performance at the macrostructural level [8–12]. The method relies on a clear separation among scales typical of multiscale systems and on expressing the fields as power series in terms of an appropriate ordering parameter related to the microscopic length scale. This approach yields to a set of recursive differential problems at the macroscale whose coefficients encode the influence of the underlying microstructure. Today, the technique is widely used to reliably investigate also complex coupled or multifield phenomena involving, for example, piezoelectricity [13–16], thermo-diffusivity [17–19], viscoelasticity [20–24], hygro-mechanics [25–27], poroelasticity [28, 29], thermo-elasticity [30–33], and electro-magneto-elasticity [34–36], to cite a few.

The recent spectro-hierarchical approach tackles the set of PDEs arising from the problem of wave propagation in periodic Cauchy materials by means of perturbative techniques, and more precisely by breaking down the equations into an infinite hierarchy of explicitly resolvable problems. The approach is extremely

*Corresponding author: francesca.fantoni@unibs.it

flexible and it has proven to be successful in radically different problems, see e.g. [37]. The smallness parameter at the core of the scheme is derived, as it is typical in the context of Nekhoroshev-type arguments, see e.g. [38–40], by the well known decay of the harmonics of real analytic functions appearing in the equation. However, this classical approach is set in a way to exploit the key property of the functions defining density and elasticity tensor, to be rapidly oscillating with a rate ε^{-1} . This ensures the right spectral separation which allows to obtain the main approximation result of [?]. It is worth recalling that the importance of this result lies in the possibility to obtain, under suitable assumptions, an approximation error of the actual solution which is superexponentially small with respect to ε^{-1} . This means that, for practical applications, the constructed solution has the potential to be “practically indistinguishable” from the real one. In this paper we show how the scheme presented in [?] can be applied to a relevant model and the way it can be employed to obtain an approximation of the solution in a fully constructive way. At the same time, the theory is tested outside the well known stringent smallness threshold for ε established by the theory. The hierarchical method reveals to be particularly effective in capturing first- and second-order contributions, thereby resolving wavefront dispersion, microstructure-induced modulations, and localized resonance phenomena that are invisible at the homogenized level, providing a richer insight into transient behavior.

Extensive numerical comparisons are carried out among the homogenized solution, the spectro-hierarchical reconstruction, and the fully heterogeneous solution, demonstrating that the hierarchical approach closely replicates the detailed, time-dependent evolution of the displacement fields across multiple instants and excitation frequencies. The results demonstrate that while asymptotic homogenization provides an efficient and reliable macroscopic approximation, the spectro-hierarchical method complements it by capturing fine-scale transient features and microstructural effects that are critical in early-time dynamics and high-frequency excitations. Another important aspect to highlight is that, while in the asymptotic homogenization technique the perturbative approximation of the governing differential equations leads to a cascade of recursive problems in which nonlocal effects are transferred to the body force, the spectro-hierarchical method results in a sequence of recursive differential problems where the body force does not increase in order with respect to that of the previous perturbative step. This feature represents a significant computational advantage. Within the asymptotic homogenization framework, the order of the body force derivative increases with the perturbative step, which may pose significant computational challenges.

The paper is structured as follows. Section 2 presents the governing equations of the elastodynamics for a periodic microstructured material. Section 3 is devoted to the illustration of the asymptotic homogenization technique for this type of material with a detailed description of the related cell problems, down-scaling and up-scaling relations and average field equations of infinite order which, appropriately truncated, lead to the field equations of the equivalent Cauchy medium. The spectro hierarchical approach is detailed in Section 4 in which the hierarchy of differential problems that is studied in the corresponding Fourier space is described. Finally, Section 5 is dedicated to the presentation of the numerical tests performed to compare the two previously described perturbative techniques by focusing on a SiC-based composite and considering both null and non-null initial conditions. Overall, the study establishes a rigorous, systematic framework that bridges homogenized models and fully heterogeneous transient dynamics, providing insights directly applicable to the design of advanced microstructured materials with controlled wave propagation, vibration mitigation, and frequency-selective behavior. This work lays the foundation for further analytical and computational studies of complex transient phenomena in engineered heterogeneous media.

2 Two-scale modeling of periodic heterogeneous elastic materials

One considers a heterogeneous medium having a periodic microstructure whose phases are modeled as linear elastic first-order continua. In a two-dimensional domain, a periodic cell $\mathcal{A} = [0, a] \times [0, \delta a]$, with $\delta \in \mathbb{R} > 0$ can be identified, having characteristic size a . Spatial repetition of micro cell \mathcal{A} along the directions of its periodicity vectors, namely $\mathbf{v}_1 = a \mathbf{e}_1$ and $\mathbf{v}_2 = \delta a \mathbf{e}_2$, allows identifying the domain $\mathcal{L} = [0, L] \times [0, \delta L]$ having structural characteristic size L . This last must be large enough so that \mathcal{L} characterizes a representative portion of the heterogeneous medium and relation $L \gg a$ must hold in order to satisfy the scales separation condition. Denoting with $\mathbf{x} = x_1 \mathbf{e}_1 + x_2 \mathbf{e}_2$ the position vector of each material point in a two-dimensional space $\{0, \mathbf{e}_1, \mathbf{e}_2\}$ and with t the time variable, in the realm of small strains local balance equation reads

$$\nabla \cdot \boldsymbol{\sigma}(\mathbf{x}, t) + \mathbf{b}(\mathbf{x}, t) = \rho^{(m,a)} \ddot{\mathbf{u}}(\mathbf{x}, t). \quad (1)$$

In equation (1), $\mathbf{u}(\mathbf{x}, t) = u_i(\mathbf{x}, t)\mathbf{e}_i$ is the micro displacement field and $\rho^{(m,a)}$ is the \mathcal{A} -periodic mass density, for which apex m is exploited to refer to the microscale. As usual, the double dot notation $(\ddot{\cdot})$ denotes the second derivative with respect to time. Body forces $\mathbf{b}(\mathbf{x}, t)$ are required to exhibit a spatial variability much greater than the micro size a in order to fulfill the scales separation requirement. Even if this is not mandatory, they are here assumed to be \mathcal{L} -periodic and to have a vanishing mean value on the structural domain \mathcal{L} . Micro stress tensor $\boldsymbol{\sigma}(\mathbf{x}, t) = \sigma_{ij}(\mathbf{x}, t)\mathbf{e}_i \otimes \mathbf{e}_j$ is constitutively related to the micro small strain tensor $\boldsymbol{\varepsilon}(\mathbf{x}, t) = \text{sym}\nabla\mathbf{u}(\mathbf{x}, t)$ through the relation

$$\boldsymbol{\sigma}(\mathbf{x}, t) = \mathbb{C}^{(m,a)}\boldsymbol{\varepsilon}(\mathbf{x}, t), \quad (2)$$

where $\mathbb{C}^{(m,a)} = C_{ijkl}^{(m,a)}\mathbf{e}_i \otimes \mathbf{e}_j \otimes \mathbf{e}_h \otimes \mathbf{e}_k$ is the \mathcal{A} -periodic fourth order micro elasticity tensor enjoying major and minor symmetries. As usually done [15, 16, 41], periodic cell \mathcal{A} can be rephrased into the unit cell $\mathcal{Q} = [0, 1] \times [0, \delta]$, this last obtained rescaling \mathcal{A} by the size a . This procedure allows to mathematically express the separation of scales through two distinct variables, namely the slow (macro) one $\mathbf{x} \in \mathcal{A}$, and the fast (micro) one $\boldsymbol{\xi} = \frac{\mathbf{x}}{a} \in \mathcal{Q}$. With this in mind, micro constitutive tensor and mass density can be defined over \mathcal{Q} as $\mathbb{C}^{(m,a)} = \mathbb{C}^m(\boldsymbol{\xi} = \frac{\mathbf{x}}{a})$ and $\rho^{(m,a)} = \rho^m(\boldsymbol{\xi} = \frac{\mathbf{x}}{a})$. Micro field equation comes from the substitution of the constitutive relation (2) into balance equation (1) and reads

$$\nabla \cdot \left(\mathbb{C}^m \left(\frac{\mathbf{x}}{a} \right) \nabla \mathbf{u}(\mathbf{x}, t) \right) + \mathbf{b}(\mathbf{x}, t) = \rho^m \left(\frac{\mathbf{x}}{a} \right) \ddot{\mathbf{u}}(\mathbf{x}, t). \quad (3)$$

In order to investigate transient problems of the kind of (3), the field equation must be equipped with appropriate initial conditions, namely

$$\mathbf{u}(\mathbf{x}, t = 0) = \mathbf{v}_0(\mathbf{x}), \quad \dot{\mathbf{u}}(\mathbf{x}, t = 0) = \mathbf{w}_0(\mathbf{x}). \quad (4)$$

Since any interface Σ between two different phases of periodic cell \mathcal{Q} is treated as perfectly bonded, micro displacement and traction vectors must satisfy the following continuity conditions

$$[[\mathbf{u}]]|_{\boldsymbol{\xi} \in \Sigma} = \mathbf{0}, \quad [[\mathbb{C}^m \nabla \mathbf{u} \cdot \mathbf{n}]]|_{\boldsymbol{\xi} \in \Sigma} = \mathbf{0}, \quad (5)$$

where symbol $[[f]]$ denotes the jump of the function f at the interface Σ and $\mathbf{n} = n_i \mathbf{e}_i$ is the outward unit normal to Σ . Introducing the dimensionless vector $\bar{\mathbf{x}} = \frac{\mathbf{x}}{L}$ and the parameter $\varepsilon = \frac{a}{L}$ that expresses the ratio between the micro and the macro characteristic lengths (and, therefore, $\varepsilon \ll 1$ for scales separation condition), micro periodic cell \mathcal{A} can be mapped in the dimensionless space into periodic cell $\bar{\mathcal{A}} = [0, \varepsilon] \times [0, \delta\varepsilon]$, whose characteristic size is ε . Spanning cell $\bar{\mathcal{A}}$ along the directions of dimensionless periodicity vectors $\bar{\mathbf{v}}_1 = \varepsilon \mathbf{e}_1$ and $\bar{\mathbf{v}}_2 = \delta\varepsilon \mathbf{e}_2$, the non dimensional structural domain $\bar{\mathcal{L}} = [0, 1] \times [0, \delta]$ can be defined in the orthogonal reference system $\{O, \bar{x}_1, \bar{x}_2\}$. Analogously to what previously done, from periodic cell $\bar{\mathcal{A}}$ it is possible to characterize unit cell $\bar{\mathcal{Q}} = [0, 1] \times [0, \delta]$ in the $\bar{\mathbf{x}}$ -space rescaling $\bar{\mathcal{A}}$ by the dimensionless characteristic size ε . Unit cell $\bar{\mathcal{Q}}$ is defined in the orthogonal reference system $\{O, \bar{\xi}_1, \bar{\xi}_2\}$, where $\bar{\boldsymbol{\xi}} = \frac{\boldsymbol{\xi}}{\varepsilon}$ represents the dimensionless fast variable. If C_r is a reference elastic stiffness and ρ_r denotes a reference mass density, one defines the following dimensionless quantities

$$\bar{t} := \frac{t}{L} \sqrt{\frac{C_r}{\rho_r}}, \quad \bar{u}_i := \frac{u_i}{L}, \quad \bar{C}_{ijkl}^m \left(\frac{\bar{\mathbf{x}}}{\varepsilon} \right) := \frac{C_{ijkl}^m \left(\frac{\mathbf{x}}{a} \right)}{C_r}, \quad \bar{\rho}^m \left(\frac{\bar{\mathbf{x}}}{\varepsilon} \right) := \frac{\rho^m \left(\frac{\mathbf{x}}{a} \right)}{\rho_r}, \quad \bar{b}_i := b_i \frac{L}{C_r}. \quad (6)$$

Differential problem (3) with initial conditions (4) transforms into

$$\begin{cases} \nabla \cdot \left(\bar{\mathbb{C}}^m \left(\frac{\bar{\mathbf{x}}}{\varepsilon} \right) \nabla \bar{\mathbf{u}}(\bar{\mathbf{x}}, \bar{t}) \right) + \bar{\mathbf{b}}(\bar{\mathbf{x}}, \bar{t}) = \bar{\rho}^m \left(\frac{\bar{\mathbf{x}}}{\varepsilon} \right) \ddot{\bar{\mathbf{u}}}(\bar{\mathbf{x}}, \bar{t}), \\ \bar{\mathbf{u}}(\bar{\mathbf{x}}, \bar{t} = 0) = \bar{\mathbf{v}}_0(\bar{\mathbf{x}}), \\ \dot{\bar{\mathbf{u}}}(\bar{\mathbf{x}}, \bar{t} = 0) = \bar{\mathbf{w}}_0(\bar{\mathbf{x}}), \end{cases} \quad (7)$$

where now symbols $\nabla(\bullet)$ and $(\ddot{\bullet})$ denote differentiation with respect to the dimensionless space and dimensionless time, respectively. Equation (7) is equipped with the relative continuity conditions

$$[[\bar{\mathbf{u}}]]|_{\bar{\boldsymbol{\xi}} \in \Sigma_1} = \mathbf{0}, \quad [[[\bar{\mathbb{C}}^m \nabla \bar{\mathbf{u}} \cdot \mathbf{n}]]]|_{\bar{\boldsymbol{\xi}} \in \Sigma_1} = \mathbf{0}, \quad (8)$$

expressing the absence of discontinuities for the displacement and traction vectors across any interface Σ_1 between two different phases in the unit cell $\bar{\mathcal{Q}}$. Because of $\bar{\mathcal{Q}}$ -periodicity of micro elasticity tensor $\bar{\mathbb{C}}^m$ and mass density $\bar{\rho}^m$ and the $\bar{\mathcal{L}}$ -periodicity of volume forces $\bar{\mathbf{b}}$, the dimensionless microscopic displacement field is such that $\bar{\mathbf{u}} = \bar{\mathbf{u}}(\bar{\mathbf{x}}, \bar{\boldsymbol{\xi}} = \frac{\bar{\mathbf{x}}}{\varepsilon}, \bar{t})$.

3 Asymptotic homogenization scheme

The asymptotic procedure delineated below allows determining the field equation of the equivalent first-order medium, that is written in terms of the dimensionless macro displacement $\bar{\mathbf{U}} = \bar{U}_i \mathbf{e}_i$ and whose overall elastic tensor and mass density are given in closed form and result to be spatially-constant. The analytical and/or computational burden of solving the PDE (3), characterized by rapidly oscillating coefficients, is thus overcome in a concise way that accurately takes into account the role of the underlying microstructure.

3.1 Asymptotic expansion of the micro displacement field, cell problems, down-scaling and up-scaling relations

According to the approach developed in [42], the contributions of the fast and slow variables in the determination of the micro displacement $\bar{\mathbf{u}}(\bar{\mathbf{x}}, \bar{\boldsymbol{\xi}} = \frac{\bar{\mathbf{x}}}{\varepsilon}, \bar{t})$ can be separated by performing an asymptotic expansion of $\bar{\mathbf{u}}$ in powers of the parameter ε (with $\varepsilon \ll 1$), namely

$$\bar{\mathbf{u}}\left(\bar{\mathbf{x}}, \bar{\boldsymbol{\xi}} = \frac{\bar{\mathbf{x}}}{\varepsilon}, \bar{t}\right) \sim \bar{\mathbf{u}}^{(0)}\left(\bar{\mathbf{x}}, \bar{\boldsymbol{\xi}} = \frac{\bar{\mathbf{x}}}{\varepsilon}, \bar{t}\right) + \varepsilon \bar{\mathbf{u}}^{(1)}\left(\bar{\mathbf{x}}, \bar{\boldsymbol{\xi}} = \frac{\bar{\mathbf{x}}}{\varepsilon}, \bar{t}\right) + O(\varepsilon^2). \quad (9)$$

Defining the total derivative of a function $g(\bar{\mathbf{x}}, \bar{\boldsymbol{\xi}}, \bar{t})$ with respect to \bar{x}_k as

$$\frac{Dg(\bar{\mathbf{x}}, \bar{\boldsymbol{\xi}} = \frac{\bar{\mathbf{x}}}{\varepsilon}, \bar{t})}{D\bar{x}_k} = \left(\frac{\partial g(\bar{\mathbf{x}}, \bar{\boldsymbol{\xi}}, \bar{t})}{\partial \bar{x}_k} + \frac{\partial g(\bar{\mathbf{x}}, \bar{\boldsymbol{\xi}}, \bar{t})}{\partial \bar{\xi}_k} \frac{\partial \bar{\xi}_k}{\partial \bar{x}_k} \right) \Bigg|_{\bar{\boldsymbol{\xi}} = \frac{\bar{\mathbf{x}}}{\varepsilon}} = \left(\frac{\partial g(\bar{\mathbf{x}}, \bar{\boldsymbol{\xi}}, \bar{t})}{\partial \bar{x}_k} + \frac{1}{\varepsilon} g_{,k} \right) \Bigg|_{\bar{\boldsymbol{\xi}} = \frac{\bar{\mathbf{x}}}{\varepsilon}}, \quad (10)$$

one has that, in view of (9), the total derivative of the component \bar{u}_h with respect to \bar{x}_k is

$$\frac{D\bar{u}_h(\bar{\mathbf{x}}, \bar{\boldsymbol{\xi}} = \frac{\bar{\mathbf{x}}}{\varepsilon}, \bar{t})}{D\bar{x}_k} = \left[\frac{\partial \bar{u}_h^{(0)}}{\partial \bar{x}_k} + \varepsilon \frac{\partial \bar{u}_h^{(1)}}{\partial \bar{x}_k} + \dots + \frac{1}{\varepsilon} \left(\bar{u}_{h,k}^{(0)} + \varepsilon \bar{u}_{h,k}^{(1)} + \dots \right) \right] \Bigg|_{\bar{\boldsymbol{\xi}} = \frac{\bar{\mathbf{x}}}{\varepsilon}}. \quad (11)$$

Initial values differential problem (3), therefore, assumes the following form, expressed componentwise, after reordering at the different orders of ε

$$\left\{ \begin{array}{l} \left(\varepsilon^{-2} \left(\bar{C}_{ijhk}^m \bar{u}_{h,k}^{(0)} \right)_{,j} + \varepsilon^{-1} \left\{ \left[\bar{C}_{ijhk}^m \left(\frac{\partial \bar{u}_h^{(0)}}{\partial \bar{x}_k} + \bar{u}_{h,k}^{(1)} \right) \right]_{,j} + \frac{\partial}{\partial \bar{x}_j} \left(\bar{C}_{ijhk}^m \bar{u}_{h,k}^{(0)} \right) \right\} + \right. \\ \left. \left[\bar{C}_{ijhk}^m \left(\frac{\partial \bar{u}_h^{(1)}}{\partial \bar{x}_k} + \bar{u}_{h,k}^{(2)} \right) \right]_{,j} + \frac{\partial}{\partial \bar{x}_j} \left[\bar{C}_{ijhk}^m \left(\frac{\partial \bar{u}_h^{(0)}}{\partial \bar{x}_k} + \bar{u}_{h,k}^{(1)} \right) \right] + \right. \\ \left. + \varepsilon \left\{ \left[\bar{C}_{ijhk}^m \left(\frac{\partial \bar{u}_h^{(2)}}{\partial \bar{x}_k} + \bar{u}_{h,k}^{(3)} \right) \right]_{,j} + \frac{\partial}{\partial \bar{x}_j} \left[\bar{C}_{ijhk}^m \left(\frac{\partial \bar{u}_h^{(1)}}{\partial \bar{x}_k} + \bar{u}_{h,k}^{(2)} \right) \right] \right\} + \right. \\ \left. - \bar{\rho}^m \frac{\partial^2 \bar{u}_i^{(0)}}{\partial \bar{t}^2} - \varepsilon \bar{\rho}^m \frac{\partial^2 \bar{u}_i^{(1)}}{\partial \bar{t}^2} + O(\varepsilon^2) \right) \Bigg|_{\bar{\boldsymbol{\xi}} = \frac{\bar{\mathbf{x}}}{\varepsilon}} + \bar{b}_i(\bar{\mathbf{x}}, \bar{t}) = 0, \\ \bar{u}_h^{(0)}(\bar{\mathbf{x}}, \bar{\boldsymbol{\xi}}, \bar{t} = 0) + \varepsilon \bar{u}_h^{(1)}(\bar{\mathbf{x}}, \bar{\boldsymbol{\xi}}, \bar{t} = 0) + O(\varepsilon^2) = \bar{v}_{h_0}(\bar{\mathbf{x}}), \\ \frac{\partial \bar{u}_h^{(0)}}{\partial \bar{t}}(\bar{\mathbf{x}}, \bar{\boldsymbol{\xi}}, \bar{t} = 0) + \varepsilon \frac{\partial \bar{u}_h^{(1)}}{\partial \bar{t}}(\bar{\mathbf{x}}, \bar{\boldsymbol{\xi}}, \bar{t} = 0) + O(\varepsilon^2) = \bar{w}_{h_0}(\bar{\mathbf{x}}). \end{array} \right. \quad (12)$$

According to the asymptotic expansion (9), also interface conditions (8) can be rewritten as

$$\begin{aligned} & \left[\left[\bar{u}_h^{(0)} \right] \right] \Bigg|_{\bar{\boldsymbol{\xi}} \in \Sigma_1} + \varepsilon \left[\left[\bar{u}_h^{(1)} \right] \right] \Bigg|_{\bar{\boldsymbol{\xi}} \in \Sigma_1} + O(\varepsilon^2) = 0, \\ & \frac{1}{\varepsilon} \left[\left[\bar{C}_{ijhk}^m \bar{u}_{h,k}^{(0)} n_j \right] \right] \Bigg|_{\bar{\boldsymbol{\xi}} \in \Sigma_1} + \left[\left[\bar{C}_{ijhk}^m \left(\frac{\partial \bar{u}_h^{(0)}}{\partial \bar{x}_k} + \bar{u}_{h,k}^{(1)} \right) n_j \right] \right] \Bigg|_{\bar{\boldsymbol{\xi}} \in \Sigma_1} + \\ & + \varepsilon \left[\left[\bar{C}_{ijhk}^m \left(\frac{\partial \bar{u}_h^{(1)}}{\partial \bar{x}_k} + \bar{u}_{h,k}^{(2)} \right) n_j \right] \right] \Bigg|_{\bar{\boldsymbol{\xi}} \in \Sigma_1} + O(\varepsilon^2) = 0. \end{aligned} \quad (13)$$

Equations (12) can be concisely rewritten as

$$\begin{cases} \varepsilon^{-2} f_i^{(0)}(\bar{\mathbf{x}}, \bar{t}) + \varepsilon^{-1} f_i^{(1)}(\bar{\mathbf{x}}, \bar{t}) + f_i^{(2)}(\bar{\mathbf{x}}, \bar{t}) + \dots + \varepsilon^l f_i^{(l+2)}(\bar{\mathbf{x}}, \bar{t}) + \bar{b}_i(\bar{\mathbf{x}}, \bar{t}) = 0, \\ \bar{u}_h^{(0)}(\bar{\mathbf{x}}, \bar{\boldsymbol{\xi}}, \bar{t} = 0) + \varepsilon \bar{u}_h^{(1)}(\bar{\mathbf{x}}, \bar{\boldsymbol{\xi}}, \bar{t} = 0) + O(\varepsilon^2) = \bar{v}_{h_0}(\bar{\mathbf{x}}), \\ \frac{\partial \bar{u}_h^{(0)}(\bar{\mathbf{x}}, \bar{\boldsymbol{\xi}}, \bar{t} = 0)}{\partial \bar{t}} + \varepsilon \frac{\partial \bar{u}_h^{(1)}(\bar{\mathbf{x}}, \bar{\boldsymbol{\xi}}, \bar{t} = 0)}{\partial \bar{t}} + O(\varepsilon^2) = \bar{w}_{h_0}(\bar{\mathbf{x}}), \end{cases} \quad (14)$$

where $f_h^{(j)}$, with $j = 0, \dots, l+2$, represent the volume forces of the relative micro differential problem and, as such, they spatially depend only on the slow variable. As detailed in Appendix 6, they are subsequently obtained imposing solvability conditions in the class of $\bar{\mathcal{Q}}$ -periodic functions. A series of non-homogeneous, elliptic differential problems in divergence form are thus derived, known as cell problems. They are here detailed up to order ε^0 , since derivation of higher-order cell problems can be obtained following the procedure here delineated without introducing further difficulties [15, 18]. Cell problems are expressed in terms of smooth, $\bar{\mathcal{Q}}$ -periodic perturbation functions (also known as micro-fluctuation functions), whose uniqueness is guaranteed by requiring them to have a vanishing mean value over $\bar{\mathcal{Q}}$, namely the condition

$$\langle (\cdot) \rangle = \frac{1}{|\bar{\mathcal{Q}}|} \int_{\bar{\mathcal{Q}}} (\cdot) d\bar{\boldsymbol{\xi}} = 0, \quad (15)$$

must hold for all perturbation functions. These last are those that take into account the role of the microstructural heterogeneity and, as such, depend upon physico-mechanical and geometrical features of the microstructure at hand. They are functions of the fast variable $\bar{\boldsymbol{\xi}}$, as well as of time. Cell problem at the order ε^{-1} and its interface conditions reads

$$\begin{aligned} & \left(\bar{C}_{ijhk}^m \bar{N}_{hpq_1, k}^{(1)} \right)_{,j} + \bar{C}_{ijpq_1, j}^m = 0, \\ & \left[\left[\bar{N}_{hpq_1}^{(1)} \right] \right] \Big|_{\bar{\boldsymbol{\xi}} \in \Sigma_1} = 0, \\ & \left[\left[\bar{C}_{ijhk}^m \left(\bar{N}_{hpq_1, k}^{(1)} + \delta_{kq_1} \delta_{hp} \right) n_j \right] \right] \Big|_{\bar{\boldsymbol{\xi}} \in \Sigma_1} = 0, \end{aligned} \quad (16)$$

where $\bar{N}_{hpq_1}^{(1)}$ is the perturbation function and symbol δ_{kq_1} stands for the Kronecker delta. Once $\bar{N}_{hpq_1}^{(1)}$ is known, at the order ε^0 , the following two cell problems can be attained, together with their interface conditions. The first one, whose perturbation function is called $\bar{N}_{hpq_1q_2}^{(2)}$, is here written in a symmetrized form with respect to indexes q_1 and q_2 and reads

$$\begin{aligned} & \left(\bar{C}_{ijhk}^m \bar{N}_{hpq_1q_2, k}^{(2)} \right)_{,j} + \frac{1}{2} \left[\left(\bar{C}_{ijhq_2}^m \bar{N}_{hpq_1}^{(1)} + \bar{C}_{ijhq_1}^m \bar{N}_{hpq_2}^{(1)} \right)_{,j} + \bar{C}_{iq_1pq_2}^m + \bar{C}_{iq_2pq_1}^m + \bar{C}_{iq_2hj}^m \bar{N}_{hpq_1, j}^{(1)} + \right. \\ & \left. + \bar{C}_{iq_1hj}^m \bar{N}_{hpq_2, j}^{(1)} \right] = \frac{1}{2} \left\langle \bar{C}_{iq_1pq_2}^m + \bar{C}_{iq_2hj}^m \bar{N}_{hpq_1, j}^{(1)} + \bar{C}_{iq_2pq_1}^m + \bar{C}_{iq_1hj}^m \bar{N}_{hpq_2, j}^{(1)} \right\rangle, \\ & \left[\left[\bar{N}_{hpq_1q_2}^{(2)} \right] \right] \Big|_{\bar{\boldsymbol{\xi}} \in \Sigma_1} = 0, \\ & \left[\left[\bar{C}_{ijhk}^m \left\{ \bar{N}_{hpq_1q_2, k}^{(2)} + \frac{1}{2} \left(\delta_{q_2k} \bar{N}_{hpq_1}^{(1)} + \delta_{q_1k} \bar{N}_{hpq_2}^{(1)} \right) \right\} n_j \right] \right] \Big|_{\bar{\boldsymbol{\xi}} \in \Sigma_1} = 0. \end{aligned} \quad (17)$$

The second cell problem arising at the order ε^0 and its interface conditions are

$$\begin{aligned} & \left(\bar{C}_{ijhk}^m \bar{N}_{hp, k}^{(2,2)} \right)_{,j} - \bar{\rho}^m \delta_{ip} = - \langle \bar{\rho}^m \rangle \delta_{ip}, \\ & \left[\left[\bar{N}_{hp}^{(2,2)} \right] \right] \Big|_{\bar{\boldsymbol{\xi}} \in \Sigma_1} = 0, \\ & \left[\left[\bar{C}_{ijhk}^m \bar{N}_{hp}^{(2,2)} n_j \right] \right] \Big|_{\bar{\boldsymbol{\xi}} \in \Sigma_1} = 0, \end{aligned} \quad (18)$$

where $\bar{N}_{hp}^{(2,2)}$ is the relative perturbation function. After solving cell problems at the different orders of ε , expansion (9) takes the form of the so-called down-scaling relation, which describes the microfield $\bar{\mathbf{u}}(\bar{\mathbf{x}}, \bar{\boldsymbol{\xi}}, \bar{t})$

in terms of the macro displacement $\bar{\mathbf{U}}(\bar{\mathbf{x}}, \bar{t})$ and its gradients through perturbation functions. Down-scaling relation makes thus evident the separation of the macro and micro variables and reads

$$\begin{aligned} \bar{u}_h(\bar{\mathbf{x}}, \bar{\boldsymbol{\xi}}, \bar{t}) &= \left[\bar{U}_h(\bar{\mathbf{x}}, \bar{t}) + \varepsilon \bar{N}_{hpq_1}^{(1)}(\bar{\boldsymbol{\xi}}, \bar{t}) \frac{\partial \bar{U}_p(\bar{\mathbf{x}}, \bar{t})}{\partial \bar{x}_{q_1}} + \right. \\ &\left. + \varepsilon^2 \left(\bar{N}_{hpq_1q_2}^{(2)}(\bar{\boldsymbol{\xi}}, \bar{t}) \frac{\partial^2 \bar{U}_p(\bar{\mathbf{x}}, \bar{t})}{\partial \bar{x}_{q_1} \partial \bar{x}_{q_2}} + \bar{N}_{hp}^{(2,2)}(\bar{\boldsymbol{\xi}}, \bar{t}) \frac{\partial^2 \bar{U}_p(\bar{\mathbf{x}}, \bar{t})}{\partial \bar{t}^2} \right) + O(\varepsilon^3) \right] \Big|_{\bar{\boldsymbol{\xi}} = \frac{\boldsymbol{\xi}}{\varepsilon}}. \end{aligned} \quad (19)$$

Macro field $\bar{\mathbf{U}}(\bar{\mathbf{x}}, \bar{t})$, in turn, is expressed in terms of the micro displacement $\bar{\mathbf{u}}(\bar{\mathbf{x}}, \bar{\boldsymbol{\xi}}, \bar{t})$ as the mean value of this last over $\bar{\mathcal{Q}}$. Accordingly, the up-scaling relation takes the form

$$\bar{U}_h(\bar{\mathbf{x}}, \bar{t}) := \langle \bar{u}_h(\bar{\mathbf{x}}, \bar{\boldsymbol{\xi}} + \bar{\boldsymbol{\zeta}}, \bar{t}) \rangle_{\bar{\boldsymbol{\zeta}}}, \quad (20)$$

where dimensionless translation variable $\bar{\boldsymbol{\zeta}} \in \bar{\mathcal{Q}}$ allows removing rapid fluctuations of coefficients [41, 43] and is such that $\varepsilon \bar{\boldsymbol{\zeta}} \in \bar{\mathcal{A}}$. For all $\bar{\mathcal{Q}}$ -periodic functions g , in fact, the following invariance property holds

$$\langle g(\bar{\boldsymbol{\xi}} + \bar{\boldsymbol{\zeta}}) \rangle_{\bar{\boldsymbol{\zeta}}} = \frac{1}{|\bar{\mathcal{Q}}|} \int_{\bar{\mathcal{Q}}} g(\bar{\boldsymbol{\xi}} + \bar{\boldsymbol{\zeta}}) d\bar{\boldsymbol{\zeta}} = \frac{1}{|\bar{\mathcal{Q}}|} \int_{\bar{\mathcal{Q}}} g(\bar{\boldsymbol{\xi}} + \bar{\boldsymbol{\zeta}}) d\bar{\boldsymbol{\xi}}. \quad (21)$$

3.2 Average field equation of infinite order

Average field equation of infinite order comes from the substitution of down-scaling relation (19) into the micro field equation (7). After reordering at the different orders of ε , it is expressed in the following form, together with initial conditions

$$\begin{cases} \bar{n}_{ipq_1q_2}^{(2)} \frac{\partial^2 \bar{U}_p}{\partial \bar{x}_{q_1} \partial \bar{x}_{q_2}} - \bar{n}^{(2,2)} \frac{\partial^2 \bar{U}_i}{\partial \bar{t}^2} + O(\varepsilon) + \bar{b}_i(\bar{\mathbf{x}}, \bar{t}) = 0, \\ \bar{U}_i(\bar{\mathbf{x}}, \bar{t} = 0) + O(\varepsilon) = \bar{v}_{0_i}(\bar{\mathbf{x}}), \\ \frac{\partial \bar{U}_i}{\partial \bar{t}}(\bar{\mathbf{x}}, \bar{t} = 0) + O(\varepsilon) = \bar{w}_{0_i}(\bar{\mathbf{x}}). \end{cases} \quad (22)$$

Coefficients $\bar{n}_{ipq_1q_2}^{(2)}$ and $\bar{n}^{(2,2)}$ of macro displacement gradients are the known terms of the relative cell problems at the order ε^0 and they are expressed as the mean value over $\bar{\mathcal{Q}}$ of linear combinations of micro elasticity tensor components, mass density, and perturbation functions. They read

$$\begin{aligned} \bar{n}_{ipq_1q_2}^{(2)} &= \frac{1}{2} \left\langle \bar{C}_{iq_2pq_1}^m + \bar{C}_{iq_2hk}^m \bar{N}_{hpq_1,k}^{(1)} + \bar{C}_{iq_1pq_2}^m + \bar{C}_{iq_1hk}^m \bar{N}_{hpq_2,k}^{(1)} \right\rangle, \\ \bar{n}^{(2,2)} &= \langle \bar{\rho}^m \rangle. \end{aligned} \quad (23)$$

In order to formally solve the average field equation of infinite order (22), one considers dimensionless macro displacement $\bar{\mathbf{U}}(\bar{\mathbf{x}}, \bar{t})$ asymptotically expanded in powers of parameter ε , namely

$$\bar{U}_i(\bar{\mathbf{x}}, \bar{t}) = \sum_{j \in \mathbb{N}} \varepsilon^j \bar{U}_i^{(j)}(\bar{\mathbf{x}}, \bar{t}). \quad (24)$$

In this way, a series of recursive macro differential problems can be obtained in terms of sensitivities $\bar{\mathbf{U}}^{(j)}$ by substituting expansion (24) into (22). They read

$$\begin{aligned} \bar{n}_{ipq_1q_2}^{(2)} \left(\frac{\partial^2 \bar{U}_p^{(0)}}{\partial \bar{x}_{q_1} \partial \bar{x}_{q_2}} + \varepsilon \frac{\partial^2 \bar{U}_p^{(1)}}{\partial \bar{x}_{q_1} \partial \bar{x}_{q_2}} + \varepsilon^2 \frac{\partial^2 \bar{U}_p^{(2)}}{\partial \bar{x}_{q_1} \partial \bar{x}_{q_2}} + \dots \right) + \\ - \bar{n}^{(2,2)} \left(\frac{\partial^2 \bar{U}_i^{(0)}}{\partial \bar{t}^2} + \varepsilon \frac{\partial^2 \bar{U}_i^{(1)}}{\partial \bar{t}^2} + \varepsilon^2 \frac{\partial^2 \bar{U}_i^{(2)}}{\partial \bar{t}^2} + \dots \right) + \dots + \bar{b}_i(\bar{\mathbf{x}}, \bar{t}) = 0. \end{aligned} \quad (25)$$

From equation (25), after reordering at the different orders of ε , one has

$$\varepsilon^0 \left(\bar{n}_{ipq_1q_2}^{(2)} \frac{\partial^2 \bar{U}_p^{(0)}}{\partial \bar{x}_{q_1} \partial \bar{x}_{q_2}} - \bar{n}^{(2,2)} \frac{\partial^2 \bar{U}_i^{(0)}}{\partial \bar{t}^2} + \bar{b}_i(\bar{\mathbf{x}}, \bar{t}) \right) + \varepsilon \left(\bar{n}_{ipq_1q_2}^{(2)} \frac{\partial^2 \bar{U}_p^{(1)}}{\partial \bar{x}_{q_1} \partial \bar{x}_{q_2}} - \bar{n}^{(2,2)} \frac{\partial^2 \bar{U}_i^{(1)}}{\partial \bar{t}^2} + \bar{b}_i^{(1)}(\bar{\mathbf{x}}, \bar{t}) \right) +$$

$$+\varepsilon^2 \left(\bar{n}_{ipq_1q_2}^{(2)} \frac{\partial^2 \bar{U}_p^{(2)}}{\partial \bar{x}_{q_1} \partial \bar{x}_{q_2}} - \bar{n}^{(2,2)} \frac{\partial^2 \bar{U}_i^{(2)}}{\partial \bar{t}^2} + \bar{b}_i^{(2)}(\bar{\mathbf{x}}, \bar{t}) \right) + O(\varepsilon^3) = 0 \quad (26)$$

At the order ε^0 , the differential problem at the macroscale is expressed in terms of the sensitivity $\bar{\mathbf{U}}^{(0)}$ and, together with its initial conditions, it reads

$$\begin{cases} \bar{n}_{ipq_1q_2}^{(2)} \frac{\partial^2 \bar{U}_p^{(0)}}{\partial \bar{x}_{q_1} \partial \bar{x}_{q_2}} - \bar{n}^{(2,2)} \frac{\partial^2 \bar{U}_i^{(0)}}{\partial \bar{t}^2} + \bar{b}_i(\bar{\mathbf{x}}, \bar{t}) = 0, \\ \bar{U}_i^{(0)}(\bar{\mathbf{x}}, \bar{t} = 0) = \bar{v}_{0_i}(\bar{\mathbf{x}}), \\ \frac{\partial \bar{U}_i^{(0)}}{\partial \bar{t}}(\bar{\mathbf{x}}, \bar{t} = 0) = \bar{w}_{0_i}(\bar{\mathbf{x}}). \end{cases} \quad (27)$$

At generic order ε^m , with $m \in \mathbb{Z}_{\geq 1}$, the governing macro differential problem can be expressed in terms of sensitivity $\bar{\mathbf{U}}^{(m)}$ as

$$\begin{cases} \bar{n}_{ipq_1q_2}^{(2)} \frac{\partial^2 \bar{U}_p^{(m)}}{\partial \bar{x}_{q_1} \partial \bar{x}_{q_2}} - \bar{n}^{(2,2)} \frac{\partial^2 \bar{U}_i^{(m)}}{\partial \bar{t}^2} + \bar{b}_i^{(m)}(\bar{\mathbf{x}}, \bar{t}) = 0, \\ \bar{U}_i^{(m)}(\bar{\mathbf{x}}, \bar{t} = 0) = 0, \\ \frac{\partial \bar{U}_i^{(m)}}{\partial \bar{t}}(\bar{\mathbf{x}}, \bar{t} = 0) = 0, \end{cases} \quad (28)$$

where $\bar{\mathbf{b}}^{(m)}$ is the known volume force vector depending on sensitivities $\bar{\mathbf{U}}^{(r)}$, with $r < m$ and on higher-order constitutive tensors $\bar{\mathbf{n}}^{(s)}$ and $\bar{\mathbf{n}}^{(s,2)}$ with $s \geq m$ arising from the average field equation of infinite order. In this way, higher-order differential problems (28) remain characterized by symmetric and positive definite constitutive tensors (the proof is given in Section 3.3). Their resolution allows for improving the solution of the heterogeneous problem since the average field equation of infinite order is asymptotically equivalent to the governing one of the heterogeneous medium, and source terms of higher-order differential problems allow taking into account non-local effects related to the microstructural length scale. If source terms are $\bar{\mathcal{L}}$ -periodic, normalization condition

$$\frac{1}{|\bar{\mathcal{L}}|} \int_{\bar{\mathcal{L}}} \bar{U}_i^{(m)}(\bar{\mathbf{x}}, \bar{t}) \, d\bar{\mathbf{x}} = 0 \quad (29)$$

needs to be satisfied $\forall m \in \mathbb{Z}$ in order to guarantee the uniqueness of the solution of the differential problem at the order ε^m . But $\bar{\mathcal{L}}$ -periodicity is not a mandatory requirement for $\bar{\mathbf{b}}^{(m)}$; if it is not satisfied appropriate boundary conditions must substitute equation (29). What is compulsory for volume forces is their independence on the micro variable $\bar{\boldsymbol{\xi}}$ in order to preserve the scales separation condition. One way to find a solution for transient macro differential problems (27)-(28) is resorting the Fourier transform [44], in order to turn partial differential equations involved in (27)-(28) into second-order ordinary differential equations in time. Fourier transform of a real-valued function $f(\bar{\mathbf{x}}, \bar{t})$ is defined as

$$\mathcal{F}(f(\bar{\mathbf{x}}, \bar{t})) := \int_{\mathbb{R}^2} f(\bar{\mathbf{x}}, \bar{t}) e^{-i \bar{\mathbf{k}} \cdot \bar{\mathbf{x}}} \, d\bar{\mathbf{x}} = \check{f}(\bar{\mathbf{k}}, \bar{t}), \quad (30)$$

where Fourier argument $\bar{\mathbf{k}} \in \mathbb{R}^2$ and i is the imaginary unit such that $i^2 = -1$. Taking into account the derivation rule $\mathcal{F}\left(\frac{\partial^n f(\bar{\mathbf{x}}, \bar{t})}{\partial \bar{x}_j^n}\right) = (i \bar{k}_j)^n \mathcal{F}(f(\bar{\mathbf{x}}, \bar{t}))$, the problem (27) is transformed into

$$\begin{cases} -\bar{k}_{q_1} \bar{k}_{q_2} \bar{n}_{ipq_1q_2}^{(2)} \check{U}_p^{(0)}(\bar{\mathbf{k}}, \bar{t}) - \bar{n}^{(2,2)} \frac{\partial^2 \check{U}_i^{(0)}(\bar{\mathbf{k}}, \bar{t})}{\partial \bar{t}^2} + \check{b}_i = 0, \\ \check{U}_i^{(0)}(\bar{\mathbf{k}}, \bar{t} = 0) = \check{v}_{0_i}(\bar{\mathbf{k}}), \\ \frac{\partial \check{U}_i^{(0)}(\bar{\mathbf{k}}, \bar{t})}{\partial \bar{t}} = \check{w}_{0_i}(\bar{\mathbf{k}}) \end{cases} \quad (31)$$

Analogously, the higher-order differential problem (28) becomes

$$\begin{cases} -\bar{k}_{q_1} \bar{k}_{q_2} \bar{n}_{ipq_1q_2}^{(2)} \check{U}_p^{(m)}(\bar{\mathbf{k}}, \bar{t}) - \bar{n}^{(2,2)} \frac{\partial^2 \check{U}_i^{(m)}(\bar{\mathbf{k}}, \bar{t})}{\partial \bar{t}^2} + \check{b}_i^{(m)} = 0, \\ \check{U}_i^{(m)}(\bar{\mathbf{k}}, \bar{t} = 0) = 0, \\ \frac{\partial \check{U}_i^{(m)}(\bar{\mathbf{k}}, \bar{t})}{\partial \bar{t}} = 0 \end{cases} \quad (32)$$

Denoting with $\check{\mathbf{r}}^{(0)} = \left[\frac{\partial \check{\mathbf{U}}^{(0)}}{\partial \bar{t}} \quad \check{\mathbf{U}}^{(0)} \right]^T$, the second-order ODE involved in (31) can be transformed into a first-order one and represented in the state space as

$$\mathbf{M} \dot{\check{\mathbf{r}}}^{(0)} + \mathbf{N}(\bar{\mathbf{k}}) \check{\mathbf{r}}^{(0)} + \mathbf{d} = \mathbf{0}. \quad (33)$$

In equation (33), \mathbf{M} is a diagonal non singular square block matrix, \mathbf{N} is a $\bar{\mathbf{k}}$ -dependent block matrix, and \mathbf{d} is a vector containing in its first block the Fourier transform of the volume force vector $\bar{\mathbf{b}}$ appearing in the zeroth-order problem (27), namely

$$\mathbf{M} = \begin{bmatrix} \mathbf{A}^{(2,2)} & \mathbf{0} \\ \mathbf{0} & \mathbf{I} \end{bmatrix}, \quad \mathbf{N}(\bar{\mathbf{k}}) = \begin{bmatrix} \mathbf{0} & \mathbf{B}^{(2)}(\bar{\mathbf{k}}) \\ -\mathbf{I} & \mathbf{0} \end{bmatrix}, \quad \mathbf{d} = \begin{bmatrix} \check{\bar{\mathbf{b}}} \\ \mathbf{0} \end{bmatrix}. \quad (34)$$

Matrices $\mathbf{A}^{(2,2)}$ and $\mathbf{B}^{(2)}(\bar{\mathbf{k}})$ are respectively expressed in terms of coefficients $\bar{n}^{(2,2)}$ and $\bar{n}_{ipq_1q_2}^{(2)}$ as

$$\mathbf{A}^{(2,2)} = - \begin{bmatrix} \bar{n}^{(2,2)} & \mathbf{0} \\ \mathbf{0} & \bar{n}^{(2,2)} \end{bmatrix}, \quad \mathbf{B}^{(2)}(\bar{\mathbf{k}}) = - \begin{bmatrix} \bar{k}_1^2 \bar{n}_{1111}^{(2)} + \bar{k}_2^2 \bar{n}_{1122}^{(2)} & 2\bar{k}_1 \bar{k}_2 \bar{n}_{1212}^{(2)} \\ 2\bar{k}_1 \bar{k}_2 \bar{n}_{2112}^{(2)} & \bar{k}_1^2 \bar{n}_{2211}^{(2)} + \bar{k}_2^2 \bar{n}_{2222}^{(2)} \end{bmatrix}. \quad (35)$$

In a completely analogous way, denoting with $\check{\mathbf{r}}^{(m)} = \left[\frac{\partial \check{\mathbf{U}}^{(m)}}{\partial \bar{t}} \quad \check{\mathbf{U}}^{(m)} \right]^T$, the ODE in (32) becomes

$$\mathbf{M} \dot{\check{\mathbf{r}}}^{(m)} + \mathbf{N}(\bar{\mathbf{k}}) \check{\mathbf{r}}^{(m)} + \mathbf{d}^{(m)} = \mathbf{0}, \quad (36)$$

with \mathbf{M} and \mathbf{N} defined as in (34), and $\mathbf{d}^{(m)}$ a vector containing in its first block the Fourier transform of volume forces $\bar{\mathbf{b}}^{(m)}$, namely $\mathbf{d}^{(m)} = \left[\check{\bar{\mathbf{b}}}^{(m)} \quad \mathbf{0} \right]^T$. The solutions $\check{\mathbf{r}}^{(0)}$ of (33) and $\check{\mathbf{r}}^{(m)}$ of (36) can formally be expressed as

$$\begin{aligned} \check{\mathbf{r}}^{(0)}(\bar{\mathbf{k}}, \bar{t}) &= \exp[-\mathbf{M}^{-1} \mathbf{N} \bar{t}] \check{\mathbf{r}}_0^{(0)}(\bar{\mathbf{k}}) + \int_0^{\bar{t}} \exp[-\mathbf{M}^{-1} \mathbf{N}(\bar{t} - \bar{\tau})] (-\mathbf{M}^{-1} \mathbf{d}) \, d\bar{\tau}, \\ \check{\mathbf{r}}^{(m)}(\bar{\mathbf{k}}, \bar{t}) &= \exp[-\mathbf{M}^{-1} \mathbf{N} \bar{t}] \check{\mathbf{r}}_0^{(m)}(\bar{\mathbf{k}}) + \int_0^{\bar{t}} \exp[-\mathbf{M}^{-1} \mathbf{N}(\bar{t} - \bar{\tau})] \left(-\mathbf{M}^{-1} \mathbf{d}^{(m)} \right) \, d\bar{\tau}, \end{aligned} \quad (37)$$

where $\exp[\cdot]$ denotes the matrix exponential, and $\check{\mathbf{r}}_0^{(0)}$ and $\check{\mathbf{r}}_0^{(m)}$ are vectors containing the Fourier transforms of the initial conditions of the relative transient problem, namely $\check{\mathbf{r}}_0^{(0)} = [\check{\bar{\mathbf{w}}}_0 \quad \check{\bar{\mathbf{v}}}_0]^T$ and $\check{\mathbf{r}}_0^{(m)} = [\mathbf{0} \quad \mathbf{0}]^T$. By applying the inverse Fourier transform

$$\mathcal{F}^{-1}(\check{f}(\bar{\mathbf{k}}, \bar{t})) := \frac{1}{(2\pi)^2} \int_{\mathbb{R}^2} \check{f}(\bar{\mathbf{k}}, \bar{t}) e^{i\bar{\mathbf{k}} \cdot \bar{\mathbf{x}}} \, d\bar{\mathbf{k}} = f(\bar{\mathbf{x}}, \bar{t}), \quad (38)$$

to equations (37), it is possible to obtain $\mathbf{r}^{(0)}(\bar{\mathbf{x}}, \bar{t})$ and $\mathbf{r}^{(m)}(\bar{\mathbf{x}}, \bar{t})$, and thus the sensitivities $\bar{\mathbf{U}}^{(j)}$ and $\partial \bar{\mathbf{U}}^{(j)} / \partial \bar{t}$ and, thanks to equation (9), reconstruct the solution at the different orders of ε . One has

$$\begin{aligned} \mathbf{r}(\bar{\mathbf{x}}, \bar{t}) &= \begin{bmatrix} \frac{\partial \bar{\mathbf{U}}}{\partial \bar{t}}(\bar{\mathbf{x}}, \bar{t}) \\ \bar{\mathbf{U}}(\bar{\mathbf{x}}, \bar{t}) \end{bmatrix} = \sum_{j \in \mathbb{N}} \varepsilon^j \left[\mathcal{F}^{-1} \left(\exp[-\mathbf{M}^{-1} \mathbf{N} \bar{t}] \right) * \mathbf{r}_0^{(j)}(\bar{\mathbf{x}}) + \right. \\ &\quad \left. + \int_0^{\bar{t}} \mathcal{F}^{-1} \left(\exp[-\mathbf{M}^{-1} \mathbf{N}(\bar{t} - \bar{\tau})] \right) * \mathcal{F}^{-1} \left(-\mathbf{M}^{-1} \mathbf{d}^{(j)} \right) \, d\bar{\tau} \right], \end{aligned} \quad (39)$$

where symbol $*$ denotes the convolution product with an appropriate tensor index contraction.

3.3 Field equation of the first-order equivalent medium

If expansion (24) is truncated at the zeroth-order, namely $\bar{\mathbf{U}}(\bar{\mathbf{x}}, \bar{t}) \approx \bar{\mathbf{U}}^{(0)}(\bar{\mathbf{x}}, \bar{t})$, and the average field equation of infinite order (22) is consistently truncated at the same order in ε , one can obtain a hyperbolic partial differential equation that is equivalent to the field equation of the first-order equivalent medium. In order to

show the formal analogy existing between the first of equations (27) and the field equation of a first-order homogenized medium, it is necessary to perform a manipulation of the first of equations (23) together with a suitable weak form of cell problem (16) at the order ε^{-1} . Specifically, the weak form can be written through multiplication of the first of equations (16) by the test function $\bar{N}_{riq_2}^{(1)}$. Thanks to the divergence theorem and $\bar{\mathcal{Q}}$ -periodicity of micro elasticity tensor and perturbation functions, the obtained weak form reads

$$\left\langle \left(\bar{C}_{rj hk}^m \bar{N}_{hpq_1, k}^{(1)} + \bar{C}_{rj pq_1}^m \right) \bar{N}_{riq_2, j}^{(1)} \right\rangle = 0. \quad (40)$$

By adding to the first of equations (23) the vanishing expression (40) and the one obtained from it exchanging indexes q_1 and q_2 , one can prove the positive definiteness of tensor $\bar{\mathbf{n}}^{(2)} = \bar{n}_{ipq_1 q_2}^{(2)} \mathbf{e}_i \otimes \mathbf{e}_p \otimes \mathbf{e}_{q_1} \otimes \mathbf{e}_{q_2} = \bar{n}_{ipq_2 q_1}^{(2)} \mathbf{e}_i \otimes \mathbf{e}_p \otimes \mathbf{e}_{q_1} \otimes \mathbf{e}_{q_2}$, as

$$\begin{aligned} \bar{n}_{ipq_1 q_2}^{(2)} &= \frac{1}{2} \left\langle \bar{C}_{rj hk}^m \left(\bar{N}_{riq_2, j}^{(1)} + \delta_{ir} \delta_{jq_2} \right) \left(\bar{N}_{hpq_1, k}^{(1)} + \delta_{ph} \delta_{kq_1} \right) + \right. \\ &\quad \left. + \bar{C}_{rj hk}^m \left(\bar{N}_{riq_1, j}^{(1)} + \delta_{ir} \delta_{jq_1} \right) \left(\bar{N}_{hpq_2, k}^{(1)} + \delta_{ph} \delta_{kq_2} \right) \right\rangle = \\ &= \frac{1}{2} \left(\bar{C}_{pq_1 iq_2} + \bar{C}_{pq_2 iq_1} \right), \end{aligned} \quad (41)$$

where $\bar{\mathbb{C}} = \bar{C}_{pq_1 iq_2} \mathbf{e}_p \otimes \mathbf{e}_{q_1} \otimes \mathbf{e}_i \otimes \mathbf{e}_{q_2}$ denotes the dimensionless overall elastic tensor. Its components can be expressed in terms of the ones of the micro elasticity tensor as

$$\bar{C}_{pq_1 iq_2} = \left\langle \bar{C}_{rj kl}^m \left(\bar{N}_{riq_2, j} + \delta_{ir} \delta_{jq_2} \right) \left(\bar{N}_{kpq_1, l} + \delta_{pk} \delta_{lq_1} \right) \right\rangle, \quad (42)$$

as inferred from equation (41). Symmetries of tensor $\bar{\mathbb{C}}$ naturally descend from the major and minor symmetry properties of the micro elasticity tensor and from equality $\bar{N}_{kpq_1}^{(1)} = \bar{N}_{kq_1 p}^{(1)}$, whose validity derives from the structure of cell problem (16). In particular, the following relation holds

$$\begin{aligned} \bar{n}_{ipq_1 q_2}^{(2)} \frac{\partial^2 \bar{U}_p}{\partial \bar{x}_{q_1} \partial \bar{x}_{q_2}} &= \frac{1}{2} \left(\bar{C}_{pq_1 iq_2} + \bar{C}_{pq_2 iq_1} \right) \frac{\partial^2 \bar{U}_p}{\partial \bar{x}_{q_1} \partial \bar{x}_{q_2}} = \\ &= \frac{1}{2} \left(\bar{C}_{pq_1 iq_2} \frac{\partial^2 \bar{U}_p}{\partial \bar{x}_{q_1} \partial \bar{x}_{q_2}} + \bar{C}_{pq_1 iq_2} \frac{\partial^2 \bar{U}_p}{\partial \bar{x}_{q_2} \partial \bar{x}_{q_1}} \right) = \bar{C}_{pq_1 iq_2} \frac{\partial^2 \bar{U}_p}{\partial \bar{x}_{q_1} \partial \bar{x}_{q_2}}, \end{aligned} \quad (43)$$

Since the equality $\bar{n}^{(2,2)} = \bar{\rho}$ between coefficient $\bar{n}^{(2,2)}$ and the overall dimensionless mass density trivially follows from the second of (23), field equation for the equivalent first-order medium and relative initial conditions become

$$\begin{cases} \bar{C}_{iq_1 pq_2} \frac{\partial^2 \bar{U}_p(\bar{\mathbf{x}}, \bar{t})}{\partial \bar{x}_{q_1} \partial \bar{x}_{q_2}} - \bar{\rho} \frac{\partial^2 \bar{U}_i(\bar{\mathbf{x}}, \bar{t})}{\partial \bar{t}^2} + \bar{b}_i(\bar{\mathbf{x}}, \bar{t}) = 0, \\ \bar{U}_i(\bar{\mathbf{x}}, \bar{t} = 0) = \bar{v}_{0i}(\bar{\mathbf{x}}), \\ \frac{\partial \bar{U}_i(\bar{\mathbf{x}}, \bar{t} = 0)}{\partial \bar{t}} = \bar{w}_{0i}(\bar{\mathbf{x}}). \end{cases} \quad (44)$$

where $\bar{\mathbf{U}}(\bar{\mathbf{x}}, \bar{t})$ can be obtained following the procedure described in the previous section. In particular, one has

$$\begin{aligned} \bar{\mathbf{U}}(\bar{\mathbf{x}}, \bar{t}) &\approx \bar{\mathbf{U}}^{(0)}(\bar{\mathbf{x}}, \bar{t}) = \left(\mathbf{Tr}^{(0)}(\bar{\mathbf{x}}, \bar{t}) \right)_2 = \left(\mathbf{T} \mathcal{F}^{-1} \left(\exp \left[-\mathbf{M}^{-1} \mathbf{N} \bar{t} \right] \right) * \mathbf{r}_0^{(0)} + \right. \\ &\quad \left. + \int_0^{\bar{t}} \mathbf{T} \mathcal{F}^{-1} \left(\exp \left[-\mathbf{M}^{-1} \mathbf{N} (\bar{t} - \bar{\tau}) \right] \right) * \mathcal{F}^{-1} \left(-\mathbf{M}^{-1} \mathbf{d} \right) d\bar{\tau}, \right)_2 \end{aligned} \quad (45)$$

where the block transformation matrix $\mathbf{T} = \mathbf{0} \oplus \mathbf{I}$ is used and where the subscript $_2$ denotes the second component of the vector. Field equation for higher-order continua cannot be simply obtained truncating equation (22) at a generic higher-order in ε , since the symmetry of non-local overall constitutive tensors, as well as the thermodynamic consistency, are not generally guaranteed [41–43]. On the contrary, to guarantee the energetic consistency of higher-order problems, different techniques based upon, for example, variational approaches can be invoked (see for instance [21, 41, 45]). They allow for consistently identifying overall non-local constitutive tensors enjoying major and minor symmetries that intervene in the constitutive law of gradient media. Variational asymptotics homogenization schemes can also be employed to consistently identify overall constitutive tensors governing the constitutive laws of multi-field first-order media (see, for example, [30, 46, 47]).

4 Spectro-hierarchical homogenization scheme

After a renormalisation of the variables, with the aim to study the problem at hand on the bi-dimensional standard torus \mathbb{T}^2 , the spectro-hierarchical scheme is described. More precisely, the known functions appearing in the equations as well as the solution are expanded according to a (well known, see, e.g. [38]) rule of selection of the Fourier harmonics (50). This leads to a hierarchy of differential problems that will be studied in the corresponding Fourier spaces.

4.1 Set-up of the method and hierarchical differential problems into Fourier coefficients

Let us consider the system (7) written in a component-wise notation, i.e.

$$\begin{cases} \rho^m(\varepsilon^{-1}\bar{\mathbf{x}})\ddot{u}_i(\bar{\mathbf{x}}, \bar{t}) - (\mathcal{C}_{ijhk}^m(\varepsilon^{-1}\bar{\mathbf{x}})\bar{u}_{h,k}(\bar{\mathbf{x}}, \bar{t}))_{,j} = \bar{b}_i(\bar{\mathbf{x}}, \bar{t}) \\ \bar{u}_i(\bar{\mathbf{x}}, \bar{t} = 0) = \bar{v}_{0_i}(\bar{\mathbf{x}}) \\ \dot{\bar{u}}_i(\bar{\mathbf{x}}, \bar{t} = 0) = w_{0_i}(\bar{\mathbf{x}}) \end{cases}, \quad (46)$$

where $\bar{\mathbf{x}} \in \bar{\mathcal{Q}}$ and the comma denotes the spatial derivative. First of all, in order to avoid a cumbersome notation but without any loss of generality, we shall set $\delta = 1$, obtaining in this way a unitary cell $\bar{\mathcal{Q}} = [0, 1] \times [0, 1]$ in the $\bar{\mathbf{x}}$ -space. By introducing the following change of variables,

$$\hat{\mathbf{x}} := 2\pi\bar{\mathbf{x}}, \quad (47)$$

the problem (46) is “reduced” to the standard torus, i.e. $\hat{\mathbf{x}} \in \hat{\mathcal{Q}} \equiv \mathbb{T}^2$. Let us now set,

$$\hat{\rho}(\varepsilon^{-1}\hat{\mathbf{x}}) := \rho^m((2\pi\varepsilon)^{-1}\bar{\mathbf{x}}), \quad \hat{\mathcal{C}}_{ijhk}(\varepsilon^{-1}\hat{\mathbf{x}}) := (2\pi)^2\mathcal{C}_{ijhk}^m((2\pi\varepsilon)^{-1}\bar{\mathbf{x}}), \quad \hat{b}_i(\hat{\mathbf{x}}) := b_i((2\pi)^{-1}\bar{\mathbf{x}}).$$

and furthermore

$$\hat{v}(\hat{\mathbf{x}}, \hat{t}) := \bar{u}((2\pi)^{-1}\bar{\mathbf{x}}, \bar{t}), \quad \hat{w}(\hat{\mathbf{x}}) := \bar{v}_0((2\pi)^{-1}\bar{\mathbf{x}}), \quad \hat{\tilde{w}}(\hat{\mathbf{x}}) := \bar{w}_0((2\pi)^{-1}\bar{\mathbf{x}}),$$

i.e. we have set $\hat{t} \equiv \bar{t}$. In this way, problem (46), reads as

$$\begin{cases} \hat{\rho}(\varepsilon^{-1}\hat{\mathbf{x}})\ddot{\hat{v}}_i(\hat{\mathbf{x}}, \hat{t}) - (\hat{\mathcal{C}}_{ijhk}(\varepsilon^{-1}\hat{\mathbf{x}})\hat{v}_{h,k}(\hat{\mathbf{x}}, \hat{t}))_{,j} = \hat{b}_i(\hat{\mathbf{x}}, \hat{t}) \\ \hat{v}_i(\hat{\mathbf{x}}, 0) = \hat{w}_i(\hat{\mathbf{x}}) \\ \dot{\hat{v}}_i(\hat{\mathbf{x}}, 0) = \hat{\tilde{w}}_i(\hat{\mathbf{x}}) \end{cases}, \quad (48)$$

where $\mathbf{x} \in \mathbb{T}^N$, with N denoting the space dimensionality.

The spectro-hierarchical approach proposed in [?] can be described as follows. Let us consider a real-analytic function, say $f(\mathbf{x})$, defined on \mathbb{T}^N . Let us recall that with the adjective real-analytic, we refer to a function $f : \mathcal{D} \rightarrow \mathbb{R}^n$ which can be extended as a holomorphic function on some complexified domain, i.e. a complex domain \mathcal{D}_σ containing the real one \mathcal{D} , where σ is a “quantification” of the extension (see [?] for an explicit definition of the analyticity radius).

Under the above-mentioned assumptions, f can be expanded via a convergent Fourier series as follows

$$f(\mathbf{x}) = \sum_{\boldsymbol{\nu} \in \mathbb{Z}^N} f_{\boldsymbol{\nu}} e^{i\boldsymbol{\nu} \cdot \mathbf{x}}. \quad (49)$$

Given two positive integers Γ and s , one can define

$$f^{[s]}(\mathbf{x}) = \sum_{(s-1)\Gamma < |\boldsymbol{\nu}| \leq s\Gamma} f_{\boldsymbol{\nu}} e^{i\boldsymbol{\nu} \cdot \mathbf{x}}. \quad (50)$$

where $|\boldsymbol{\nu}| := |\nu_1| + \dots + |\nu_N|$. Clearly, as (49) is convergent, $f = f^{[0]} + f^{[1]} + f^{[2]} + \dots$ and this holds for all $\Gamma > 0$ (where $f^{[0]} := f_0$ i.e. the average of f). It is a standard result from the theory of real-analytic functions that the size of the $f^{[s]}$ decays as $\tilde{\lambda}^s$, where $\tilde{\lambda} \in (0, 1)$ is some parameter which can be computed

explicitly. Following this property, it is customary in Perturbation Theory to rewrite the previous sum as $f = f^{[0]} + \lambda f^{[1]} + \lambda^2 f^{[2]} + \dots$ where λ is thought as one throughout the whole process, i.e. its only role is to provide a “label” for the terms $f^{[s]}$. Clearly, those terms will depend upon Γ . Exactly as in similar approaches in finite dimension, see e.g. [38], it is possible to show that a best choice for this parameter exists. More on this aspect later.

Let us proceed then by expanding the known terms appearing in (48) in the following form

$$\hat{\rho} = \hat{\rho}^{[0]} + \lambda \hat{\rho}^{[1]} + \lambda^2 \hat{\rho}^{[2]} + \dots \quad (51)$$

$$\mathcal{C}_{ijhk} = \hat{C}_{ijhk}^{[0]} + \lambda \hat{C}_{ijhk}^{[1]} + \lambda^2 \hat{C}_{ijhk}^{[2]} + \dots \quad (52)$$

$$\hat{b}_i = \lambda \hat{b}_i^{[1]} + \lambda^2 \hat{b}_i^{[2]} + \lambda^3 \hat{b}_i^{[3]} + \dots \quad (53)$$

(the choice of a zero-averaging source is customary in this class of problems) and a similar expansion holds for the initial conditions, for instance, $\hat{w}_i = \hat{w}_i^{[0]} + \lambda \hat{w}_i^{[1]} + \dots$

Accordingly, the solution to (48) is sought of the form

$$\hat{v}_i = \lambda \hat{v}_i^{[1]} + \lambda^2 \hat{v}_i^{[2]} + \lambda^3 \hat{v}_i^{[3]} + \dots \quad (54)$$

By substituting the expansions (51), (52), (53), and (54) in (48) one gets, in particular

$$\left(\hat{\rho}^{[0]} + \lambda \hat{\rho}^{[1]} + \lambda^2 \hat{\rho}^{[2]} + \dots \right) \partial_{tt} \left(\lambda \hat{v}_i^{[1]} + \lambda^2 \hat{v}_i^{[2]} + \lambda^3 \hat{v}_i^{[3]} + \dots \right) + \quad (55)$$

$$- \left[\left(\hat{C}_{ijhk}^{[0]} + \lambda \hat{C}_{ijhk}^{[1]} + \lambda^2 \hat{C}_{ijhk}^{[2]} + \dots \right) \left(\lambda \hat{v}_i^{[1]} + \lambda^2 \hat{v}_i^{[2]} + \lambda^3 \hat{v}_i^{[3]} + \dots \right) \right]_{,k} \Big|_{,j} = \lambda \hat{b}_i^{[1]} + \lambda^2 \hat{b}_i^{[2]} + \lambda^3 \hat{b}_i^{[3]} + \dots \quad (56)$$

It is now sufficient to compare the terms “labelled” with the same power of λ , to transform (48) into an infinite hierarchy of differential problems, which, remarkably, have an explicit form. A similar procedure is used for the initial conditions. For instance, by comparing the first powers of λ , one gets

Order one

$$\begin{cases} \hat{\rho}^{[0]} \ddot{\hat{v}}_i^{[1]} - \hat{C}_{ijhk}^{[0]} \left(\hat{v}_{h,k}^{[1]} \right)_{,j} = \hat{b}_i^{[1]} \\ \hat{v}_i^{[1]}(\hat{\mathbf{x}}, 0) = \hat{w}_i^{[1]}(\hat{\mathbf{x}}) \\ \dot{\hat{v}}_i^{[1]}(\hat{\mathbf{x}}, 0) = \tilde{\hat{w}}_i^{[1]}(\hat{\mathbf{x}}) \end{cases} \quad (57)$$

Order two

$$\begin{cases} \hat{\rho}^{[0]} \ddot{\hat{v}}_i^{[2]} - \hat{C}_{ijhk}^{[0]} \left(\hat{v}_{h,k}^{[2]} \right)_{,j} = \hat{b}_i^{[2]} - \hat{\rho}^{[1]} \ddot{\hat{v}}_i^{[1]} + \left(\hat{C}_{ijhk}^{[1]} \hat{v}_{h,k}^{[1]} \right)_{,j} \\ \hat{v}_i^{[2]}(\hat{\mathbf{x}}, 0) = \hat{w}_i^{[2]}(\hat{\mathbf{x}}) \\ \dot{\hat{v}}_i^{[2]}(\hat{\mathbf{x}}, 0) = \tilde{\hat{w}}_i^{[2]}(\hat{\mathbf{x}}) \end{cases} \quad (58)$$

Order three

$$\begin{cases} \hat{\rho}^{[0]} \ddot{\hat{v}}_i^{[3]} - \hat{C}_{ijhk}^{[0]} \left(\hat{v}_{h,k}^{[3]} \right)_{,j} = \hat{b}_i^{[3]} - \hat{\rho}^{[2]} \ddot{\hat{v}}_i^{[1]} - \hat{\rho}^{[1]} \ddot{\hat{v}}_i^{[2]} + \left(\hat{C}_{ijhk}^{[2]} \hat{v}_{h,k}^{[1]} + \hat{C}_{ijhk}^{[1]} \hat{v}_{h,k}^{[2]} \right)_{,j} \\ \hat{v}_i^{[3]}(\hat{\mathbf{x}}, 0) = \hat{w}_i^{[3]}(\hat{\mathbf{x}}) \\ \dot{\hat{v}}_i^{[3]}(\hat{\mathbf{x}}, 0) = \tilde{\hat{w}}_i^{[3]}(\hat{\mathbf{x}}) \end{cases} \quad (59)$$

In general, the s -th step of the hierarchy, has the form

$$\begin{cases} \hat{\rho}^{[0]} \ddot{\hat{v}}_i^{[s]} - \hat{C}_{ijhk}^{[0]} \left(\hat{v}_{h,k}^{[s]} \right)_{,j} = \hat{b}_i^{[s]} + \hat{F}_i^{[s]} \\ \hat{v}_i^{[s]}(\hat{\mathbf{x}}, 0) = \hat{w}_i^{[s]}(\hat{\mathbf{x}}) \\ \dot{\hat{v}}_i^{[s]}(\hat{\mathbf{x}}, 0) = \tilde{\hat{w}}_i^{[s]}(\hat{\mathbf{x}}) \end{cases} \quad (60)$$

where $\hat{F}_i^{[s]}$ is a suitable function representing the contribution of the solutions $\hat{v}_i^{[s-1]}, \dots, \hat{v}_i^{[1]}$ determined by to the previous stages of the hierarchy, see [?] for the general proof. This implies that the problems (60) are fully explicit.

The very first step of the scheme, i.e. for $s = 1$, should be interpreted as the “step zero” i.e. related to the “fully homogenized” problem, being the rapidly oscillating functions replaced by their average.

Clearly, the most natural question concerns the behaviour of the series (54) as their order is increased, that is, when one is interested in solving (60) as s becomes larger and larger. Classical results from Perturbation Theory show how those series, at least generically, fail to converge. This means that the function

$$\hat{v}_i^{[\leq n]} = \lambda \hat{v}_i^{[1]} + \lambda^2 \hat{v}_i^{[2]} + \dots + \lambda^n \hat{v}_i^{[n]},$$

will not provide, in general, a better approximation of $\hat{v}_i^{[\leq (n-1)]}$, even if n is “not that large”. Nevertheless, in the very same spirit of the Nekhoroshev Theorem, see e.g. [48], [49] and [50], the result contained in [?] shows that, under some reasonable assumptions, there exists an optimal n^* providing the best approximation of the exact solution amongst all the possible values of n . Remarkably, such an approximation is “extremely good”: the approximated solution $\hat{v}_i^{[\leq n^*]}$ produced with the above-described scheme is shown to be superexponentially close in ε to the exact solution. More precisely, there exists two positive constants $\mathfrak{A}, \mathfrak{a} > 0$ such that, if \hat{v} denotes the exact solution, one has

$$\left\| \hat{v} - \hat{v}^{[\leq n^*]} \right\|_* \leq \mathfrak{A} \exp(-\mathfrak{A} \exp(\mathfrak{a}/\varepsilon)^{1/4}),$$

where $\|\cdot\|_*$ is a suitable norm, see [?] for more details.

As it is common in rigorous perturbative arguments, the result of [?] are shown to hold for $\varepsilon < \varepsilon_0$, where the threshold ε_0 is estimated as a “very small” number, see [?, Formula (51)] for an explicit bound. Clearly this kind of condition are sufficient but not necessary. Hence, the purpose of this work is to attempt a validation of the approximation provided by the scheme for a value of ε far larger than the one computed via the analytic approach described in [?].

4.2 General procedure of application of the scheme

The aim of this section is to give a description of the spectro-hierarchical approach in its full generality. The described computations will be carried out in full detail for a concrete example in the next section.

First of all, as anticipated in the foreword, the results contained in [?], deal with models in which the known terms, and more precisely $\hat{\rho}, \hat{\mathcal{C}}_{ijhk}, \hat{b}_i, \hat{w}_i, \hat{w}_i$, are supposed to be, in fact, real-analytic functions. We stress, however, that “realistic” functions, say $\hat{\rho}^r$ and $\hat{\mathcal{C}}_{ijhk}^r$, do not satisfy this regularity requirement, at least in general realistic applications. In fact, they usually vary, without being even continuous, from a minimum to a maximum value and vice-versa. More precisely, $\hat{\rho}^r$ will jump from $\hat{\rho}_a$ and $\hat{\rho}_b$ ($\hat{\rho}_a < \hat{\rho}_b$) as \hat{x} vary, according to a prescribed law. The same holds for $\hat{\mathcal{C}}_{ijhk}^r$, where the two (families of) extreme values are given by $\hat{\mathcal{C}}_{ijhk}^a$ and $\hat{\mathcal{C}}_{ijhk}^b$.

Nevertheless, it is well known that several techniques can be found in the literature in order to produce real-analytic approximants of the described functions. Perhaps, the most natural approach consists in using the truncated Fourier expansion, either directly computed from original function or from other ad hoc “smoothed” ones, as the one used later on.

Let us now suppose that $\hat{\rho}, \hat{\mathcal{C}}_{ijhk}$ are either real-analytic functions or real-analytic approximants of functions $\hat{\rho}^r$ and $\hat{\mathcal{C}}_{ijhk}^r$, respectively. Let be σ their analyticity radius. According to [?, Thm. 1], we set

$$\Gamma \geq \Gamma^* := \lceil 2/\sigma \rceil. \quad (61)$$

(here $\lceil a \rceil$ denotes the smallest integer greater or equal than a), under the condition

$$1/(\varepsilon\Gamma) = 1, 2, \dots, \quad (62)$$

i.e. a non negative integer. As ε is related to the geometry of the material, not all the values of ε are possible, there is however some freedom in the admissible values, as Γ is not fixed but it can be increased if necessary. We shall call feasible, a material in which the value of ε satisfies condition (62). It is worth pointing out that, in order for the quantitative estimates of [?, Thm. 1] to hold, such an ε has to satisfy certain additional smallness requirement. However, as mentioned before, our aim is to investigate the accuracy of the method outside the theory provided by [?, Thm. 1], by providing a numerical validation. Hence, we will not impose any further restriction on ε in this case.

Once the choice (61) has been made, the functions appearing in the expansions (51) – (53) (constructed via the Fourier coefficients collection described in definition (50)) are uniquely defined. As in [?], we will choose the initial conditions in such a way $\hat{\mathbf{w}} \equiv \hat{\mathbf{w}}^{[1]}$ and $\tilde{\mathbf{w}} \equiv \tilde{\mathbf{w}}^{[1]}$. This is not a particularly restrictive choice, as Γ is typically a “large” number.

In this setting, we can start by solving the equations of the hierarchy (60). A comment is in order on the procedure used to deal with problems of the form (60). Let us recall for this purpose that a standard approach consists of proceeding with a Fourier expansion of the functions appearing in it, then solving the obtained family of finite-dimensional Cauchy problems. More precisely, as in [?], we expand

$$\hat{\mathbf{v}}^{[s]} =: \sum_{\nu \in \mathbb{Z}^N} \mathbf{c}_\nu^{[s]}(\hat{t}) e^{i\nu \cdot \hat{\mathbf{x}}}, \quad (63)$$

i.e. $\mathbf{c}_\nu^{[s]}$ denote the Fourier coefficients of $\hat{\mathbf{v}}^{[s]}$. Similarly, we denote with $\mathbf{g}_\nu^{[s]}(\hat{t})$, $\mathbf{f}_\nu^{1,[s]}$ and $\mathbf{f}_\nu^{2,[s]}$ the Fourier coefficients of $\hat{\mathbf{b}}^{[s]} + \hat{\mathbf{F}}^{[s]}$, $\hat{\mathbf{w}}^{[s]}$ and of $\tilde{\mathbf{w}}^{[s]}$, respectively.

This leads to the following infinite set of ODEs

$$\begin{cases} \hat{\rho}^{[0]} \dot{\mathbf{c}}_\nu^{[s]} + \Delta_\nu \mathbf{c}_\nu^{[s]} = \mathbf{g}_\nu^{[s]} \\ \mathbf{c}_\nu(0) = \mathbf{f}_\nu^{1,[s]} \\ \dot{\mathbf{c}}_\nu(0) = \mathbf{f}_\nu^{2,[s]} \end{cases}. \quad (64)$$

Here Δ_ν represents a 2×2 matrix whose component ih is expressed as $\left(\nu_j \nu_k C_{ijhk}^{[0]} \right)_{ih}$. The latter is positive definite as a consequence of the assumptions. It should be stressed that, with the exception of very special cases in which Δ_ν is diagonal, the solution of (64) would require a coordinates change. More precisely, the (standard) procedure can be described as follows (see also [?], Prop. 4.2):

Due to the mentioned properties of Δ_ν there exists an orthonormal matrix $\tilde{\mathbf{P}}$ such that

$$\mathbf{P}^T \Delta_\nu \mathbf{P} = \mathbf{\Lambda},$$

where $\mathbf{\Lambda} := \text{diag}(\lambda_1, \lambda_2)$. Hence, by considering the coordinates transformation given by

$$\mathbf{c}_\nu^{[s]} =: \mathbf{P} \mathbf{z}_\nu^{[s]} \quad (65)$$

the problem (64) is cast into the system of uncoupled Cauchy problems

$$\begin{cases} \ddot{\mathbf{z}}_\nu^{[s]} + \tilde{\mathbf{\Lambda}} \mathbf{z}_\nu^{[s]} = \tilde{\mathbf{P}}^T \mathbf{g}_\nu^{[s]} \\ \mathbf{z}_\nu^{[s]}(0) = \tilde{\mathbf{P}}^T \mathbf{f}_\nu^{1,[s]} \\ \dot{\mathbf{z}}_\nu^{[s]}(0) = \tilde{\mathbf{P}}^T \mathbf{f}_\nu^{2,[s]} \end{cases}, \quad (66)$$

where $\tilde{\mathbf{\Lambda}} := (\hat{\rho}^{[0]})^{-1} \mathbf{\Lambda}$ and similarly for $\tilde{\mathbf{P}}$.

The solution to the previous problem is readily written as

$$(z_\nu)_i^{[s]}(\hat{t}) = (\tilde{\mathbf{P}}^T \mathbf{f}_\nu^{1,[s]})_i \cos(\tilde{\lambda}_i^{1/2} \hat{t}) + (\tilde{\mathbf{P}}^T \mathbf{f}_\nu^{2,[s]})_i \sin(\tilde{\lambda}_i^{1/2} \hat{t}) + \tilde{\lambda}_i^{-1/2} \int_0^{\hat{t}} (\tilde{\mathbf{P}}^T \mathbf{g}_\nu^{[s]}(\tau))_i \sin[\tilde{\lambda}_i^{1/2}(\hat{t} - \tau)] d\tau, \quad (67)$$

which gives the solution to the original problem via (65). Here $\tilde{\lambda}_i$ denote the elements of $\tilde{\mathbf{\Lambda}}$.

In conclusion, the procedure can be summarised as follows

1. Consider real-analytic functions $\hat{\rho}$ and \hat{C}_{ijhk} representing the “material” (possibly as approximants of some functions $\hat{\rho}^r$ and \hat{C}_{ijhk}^r , respectively). Let be σ their analyticity radius.
2. Check if the material is feasible according to the definition given above, i.e., whether or not ε satisfies condition (62) (possibly adjusting the value of Γ within the limitation (61)). If yes, then proceed.
3. Set a “normalisation order” n

4. Consider a zero averaging source $\hat{\mathbf{b}}$ and its Fourier expansion together with those of $\hat{\rho}$ and $\hat{\mathcal{C}}_{ijhk}$ up to the harmonics such that $|\boldsymbol{\nu}| \leq n\Gamma$. This gives rise to the expansions (51)-(53), via (50). Define a set of initial conditions such that $\hat{\mathbf{w}} \equiv \hat{\mathbf{w}}^{[1]}$ and $\hat{\mathbf{v}} \equiv \hat{\mathbf{v}}^{[1]}$.
5. For all $s \leq n$ compute the corresponding $\hat{\mathbf{F}}^{[s]}$ (recall that $\hat{\mathbf{F}}^{[s]} \equiv \mathbf{0}$) then solve the Cauchy problem (60).

Remark 4.1. The normalisation order mentioned in step 3 is “automatically determined” by the original scheme in order to achieve the superexponential bound. Cases in which the theory is tested outside the rigorous validity threshold for ε , as the present one, are necessarily concerned with an arbitrary choice of n .

5 Illustrative examples-benchmark tests

One considers a microstructured material characterized by a periodic cell as the one depicted in figure 1-(a). The inclusion is made of Silicon Carbide with Young Modulus $E^{SiC} = 340$ GPa, Poisson’s ration $\nu^{SiC} = 0.18$, and mass density $\rho^{SiC} = 3210$ kg/m³. Under plane stress conditions, the elastic tensor of the inclusion reads

$$\mathbb{C}^{SiC} = \begin{pmatrix} 36.917 & 8.104 & 0 \\ 8.104 & 36.917 & 0 \\ 0 & 0 & 14.407 \end{pmatrix} 10^4 \text{ MPa.} \quad (68)$$

Without losing generality, the components of the elastic tensor of the matrix are considered as equal to 1/3 of the corresponding ones of the inclusion, and the same ratio has been taken for the mass density. Let us define the following function

$$\begin{aligned} \mathcal{M}(\xi_1, \xi_2; r^-, r^+) &= r^- + \frac{r^+ - r^-}{4} \left(\tanh \left[\frac{\cos(2\pi\xi_1/L) + w}{\alpha} \right] - \tanh \left[\frac{\cos(\pi/L) + w}{\alpha} \right] \right) \times \\ &\times \left(\tanh \left[\frac{\cos(2\pi\xi_2/L) + w}{\alpha} \right] - \tanh \left[\frac{\cos(\pi/L) + w}{\alpha} \right] \right), \end{aligned} \quad (69)$$

where r^- and r^+ are its minimum and its maximum value, respectively. The parameter α is meant to be “small but not zero” as it controls the real-analyticity radius σ of the function. More precisely, it is possible to show that

$$\sigma < \arccos(i\pi\alpha/2 - w). \quad (70)$$

The parameter w governs the size of the inclusion. Both α and w will be chosen equal to 0.1. The material addressed is supposed to have elastic constitutive properties and mass density obeying the following laws inside the periodic unit cell \mathcal{Q} (see figure 1-(b))

$$\mathcal{C}_{ijhk} := \mathcal{M}(\xi_1, \xi_2; \mathcal{C}_{ijhk}^a, \mathcal{C}_{ijhk}^b), \quad \rho := \mathcal{M}(\xi_1, \xi_2; \rho^a, \rho^b), \quad (71)$$

where apex a refer to the matrix, and b to the inclusion. Because of the \mathcal{Q} -periodicity of function (69), its

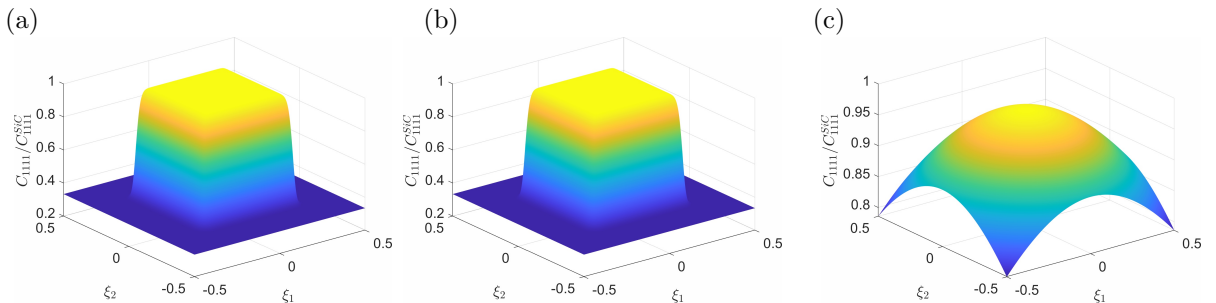


Figure 1: Plot of the dimensionless component C_{1111}/C_{1111}^{SiC} of the elastic tensor inside the unit periodic cell considering a square inclusion (a), a material whose constitutive properties obey equation (69) (b), and a material whose constitutive properties behaves as (72) (c).

multidimensional Fourier series truncated at the first order has been taken into account (see figure 1-(c)). It reads

$$\mathcal{M}(\xi_1, \xi_2, r^-, r^+) \sim c_{00} + c_{10} \cos(2\pi\xi_1) + c_{01} \cos(2\pi\xi_2), \quad (72)$$

with Fourier coefficients expressed as

$$c_{00} = \int_{\mathcal{Q}} \mathcal{M}(\xi_1, \xi_2, r^-, r^+) d\xi, \quad c_{10} = \int_{\mathcal{Q}} \mathcal{M}(\xi_1, \xi_2, r^-, r^+) \cos(2\pi\xi_1) d\xi, \quad c_{01} = \int_{\mathcal{Q}} \mathcal{M}(\xi_1, \xi_2, r^-, r^+) \cos(2\pi\xi_2) d\xi. \quad (73)$$

The periodic medium has been subjected to zero-averaging volume forces expressed as

$$\mathbf{b} = \left[\Omega \sin\left(\frac{2\pi x_1}{L} - \theta t\right) \ 0 \right]^T, \quad (74)$$

where $\Omega \in \mathbb{R}_{>0}$. Furthermore, because of the invariance of (74) with respect to x_2 , the heterogeneous medium has been discretized exploiting a standard finite element procedure considering a cluster of cells made of 21 cells along the x_1 direction and 1 cell along the x_2 direction. The initial conditions will be set as

$$\text{Case 1:} \quad \mathbf{v}_0 := (M \sin(2\pi L^{-1} x_1), 0) \quad \mathbf{w}_0 := (-M \cos(2\pi L^{-1} x_1), 0), \quad (75)$$

$$\text{Case 2:} \quad \mathbf{v}_0 := \mathbf{0} \quad \mathbf{w}_0 := \mathbf{0}, \quad (76)$$

where $M \in \mathbb{R}_{>0}$. The solution of the transient problem for the heterogeneous medium will be compared later on with the homogenized one obtained with the asymptotic homogenization technique described in Section 3 and with the one provided by the spectro-hierarchical homogenization scheme presented in Section 4.

5.1 Asymptotic approach

To assess the capabilities of the first-order asymptotic homogenization scheme described in Section 3 in solving multiscale transient problems for periodic microstructured Cauchy materials, the formulation is tested in the case of two-dimensional infinite elastic material subjected to \mathcal{L} -periodic body forces (74), with initial conditions (75) or (76). Considering that the components of the elastic tensor and the mass density of the periodic cell vary following the law given by (72), perturbation functions $\bar{N}_{hpq_1}^{(1)}$ have been derived through the numerical resolution of cell problems (16) at the order ε^{-1} discretizing the unit cell $\bar{\mathcal{Q}}$ by a standard finite element procedure. Two of the obtained perturbation functions are plotted in figure 2, which confirms their $\bar{\mathcal{Q}}$ -periodicity and their smoothness along the boundaries of the cell. Furthermore, perturbation functions are zero-average functions over $\bar{\mathcal{Q}}$ because of the imposed normalization condition (15). Once the perturbation

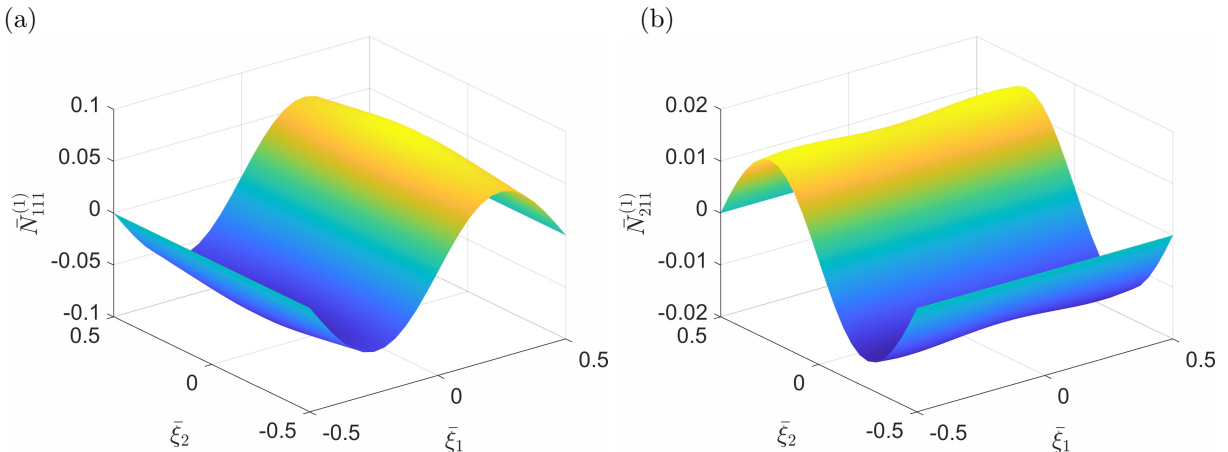


Figure 2: Perturbation functions $\bar{N}_{111}^{(1)}$ (a) and $\bar{N}_{211}^{(1)}$ (b), as solutions of cell problem (16).

functions are known, the components of the overall elastic tensor $\bar{\mathbb{C}}$ are computed through equation (42) and read

$$\bar{\mathbb{C}} = \begin{pmatrix} 0.4633 & 0.0901 & 0 \\ 0.0901 & 0.4633 & 0 \\ 0 & 0 & 0.1765 \end{pmatrix}, \quad (77)$$

where the reference elastic stiffness C_r is taken equal to C_{1111}^{SiC} . The overall dimensionless mass density $\bar{\rho}$, results equal to 0.5220 from the second of (23), where the reference mass density ρ_r is taken equal to ρ^{SiC} .

5.2 Spectro-hierarchical approach

In this section, the dimensional counterparts of the object involved in the procedure are reported, in line with the notation used for (69). This has the aim of offering a more expressive presentation of the results as well as an immediate comparison with the plots reported. The steps outlined at the end of Section 4.2 will be detailed in the following.

Steps 2 and 3:

By choosing, for instance, $\alpha = 0.1$, we shall set $\sigma = 0.0975 < 0.15644$, where the latter is obtained directly from (70). Hence, $\Gamma \equiv \Gamma^* := \lceil 2/\sigma \rceil = 21$. We will choose $\varepsilon = 1/21$, so that the material considered is feasible according to the definition given before. We set $n = 2$.

Steps 4 and 5:

Let us recall the expression of $\mathcal{M}(\hat{x}_1, \hat{x}_2; r^-, r^+)$ given in (69). By symmetry, its first order Fourier expansion reads as

$$\mathcal{M}(\hat{x}_1, \hat{x}_2; r^-, r^+) \sim r^- + c_0(r^+ - r^-) + c_1(r^+ - r^-) \left[\cos\left(\frac{\hat{x}_1}{\varepsilon}\right) + \cos\left(\frac{\hat{x}_2}{\varepsilon}\right) \right], \quad (78)$$

where c_0 and c_1 are numerically determined coefficients obtained by setting $\alpha = w = 0.1$. Hence, we will now consider the following (truncated) expansions

$$\begin{aligned} \hat{\rho} &= \hat{\rho}^{[0]} + \hat{\rho}^{[1]}, \\ \hat{C}_{ijhk} &= \hat{C}_{ijhk}^{[0]} + \hat{C}_{ijhk}^{[1]}, \end{aligned} \quad (79)$$

where

$$\begin{aligned} \hat{\rho}^{[0]} &:= \hat{\rho}^a + c_0(\hat{\rho}^b - \hat{\rho}^a), & \hat{\rho}^{[1]} &:= c_1(\hat{\rho}^b - \hat{\rho}^a) \left[\cos\left(\frac{\hat{x}_1}{\varepsilon}\right) + \cos\left(\frac{\hat{x}_2}{\varepsilon}\right) \right], \\ \hat{C}_{ijhk}^{[0]} &:= \hat{C}_{ijhk}^a + c_0(\hat{C}_{ijhk}^b - \hat{C}_{ijhk}^a), & \hat{C}_{ijhk}^{[1]} &:= c_1(\hat{C}_{ijhk}^b - \hat{C}_{ijhk}^a) \left[\cos\left(\frac{\hat{x}_1}{\varepsilon}\right) + \cos\left(\frac{\hat{x}_2}{\varepsilon}\right) \right]. \end{aligned} \quad (80)$$

We will choose the prototype (74) of (zero-averaging) source with the case studies described in (75) and (76). Let us finally introduce the following notation for the nonvanishing components of the tensor $C_{ijhk}^{[0]}$:

$$A^{[j]} := \hat{C}_{1111}^{[j]} \equiv \hat{C}_{2222}^{[j]}, \quad B^{[j]} := \hat{C}_{1122}^{[j]}, \quad C^{[j]} := \hat{C}_{1212}^{[j]}, \quad (81)$$

as they will be used later on.

Order one

As a consequence of the special choice for (74), we can carry out the computations concerning the first step in an exceptionally simple way. In particular, the only non-trivial problem involves the first component $v_1^{[1]}$ of the solution vector, as it is immediate to realise that the component $v_2^{[1]}$ is identically zero. We shall solve the initial-values problem for $s = 1$ for the case study 1, being the second an easier particular case.

$$\begin{cases} \hat{\rho}^{[0]} \ddot{v}_1^{[1]} - A^{[0]} \hat{v}_1^{[1]} = \Omega \sin(\hat{x}_1 - \hat{\theta} \hat{t}) \\ \hat{v}_1^{[1]}(\hat{\mathbf{x}}, 0) = M \sin(\hat{x}_1) \\ \dot{\hat{v}}_1^{[1]}(\hat{\mathbf{x}}, 0) = -M \cos(\hat{x}_1) \end{cases} \quad (82)$$

The solution to this special model is given immediately by Duhamel's formula

$$\begin{aligned} \hat{v}_1^{[1]}(\hat{x}_1, \hat{t}) &= \frac{M}{2} \left[\sin(\hat{x}_1 + 2\pi \hat{t}) + \sin(\hat{x}_1 - 2\pi \hat{t}) \right] - \frac{ML}{4\pi c} \int_{\hat{x}_1 - 2\pi \hat{t}}^{\hat{x}_1 + 2\pi \hat{t}} \cos(\hat{y}_1) d\hat{y}_1 + \\ &- \frac{\Omega L^2}{2\pi c r_0} \int_0^{\hat{t}} \int_{\hat{x}_1 - 2\pi(\hat{t} - \hat{\tau})}^{\hat{x}_1 + 2\pi(\hat{t} - \hat{\tau})} \sin(\hat{\tau} \hat{\theta} - \hat{y}_1) d\hat{y}_1 d\hat{\tau}, \end{aligned} \quad (83)$$

where we have set $c := \sqrt{A^{[0]}/\hat{\rho}^{[0]}}$, clearly subject to the non-resonance condition $\hat{\theta} \neq 2\pi$.

The solution corresponding to case study 2, holding under the same condition, is straightforwardly obtained from the previous one simply by setting $M = 0$.

Order two

Let us now write system (58) explicitly. It is worthy to stress that the special properties $\hat{u}_1 = \hat{u}_1(\hat{x}_1, \hat{t})$ and $\hat{u}_2 \equiv 0$ simplify the r.h.s. remarkably. The whole system, subject to null initial conditions, reads as

$$\begin{cases} \hat{\rho}^{[0]}\ddot{\hat{v}}_1^{[2]} - \mathcal{D}_1^{(0)}\{\hat{v}_1^{[2]}, \hat{v}_2^{[2]}\} = A^{[1]}\hat{v}_{1,11}^{[1]} + \left(A^{[1]}\hat{v}_{1,1}^{[1]}\right)_{,1} - \hat{\rho}^{[1]}\ddot{\hat{v}}_1^{[1]} \\ \hat{\rho}^{[0]}\ddot{\hat{v}}_2^{[2]} - \mathcal{D}_2^{(0)}\{\hat{v}_1^{[2]}, \hat{v}_2^{[2]}\} = \left(B^{[1]}\hat{v}_{1,1}^{[1]}\right)_{,2} \end{cases} \quad (84)$$

where the spatial operator

$$\mathcal{D}^{(0)}\{f, g\} := \left((A^{(0)}f_{,11} + \Gamma^{(0)}f_{,22}) + (B^{(0)} + \Gamma^{(0)})g_{,12}, (B^{(0)} + \Gamma^{(0)})f_{,12} + (\Gamma^{(0)}g_{,11} + A^{(0)}g_{,22}) \right), \quad (85)$$

appears at any stage of the hierarchy as well as the whole structure of the l.h.s. described in (84). It is easy to realise that the r.h.s. of (84), which can be immediately computed from (58) via (80), (81) and the above found $v_1^{[1]}$, is quite cumbersome and it's not reported here. However, as already described in Sec. 4.2, these r.h.s., namely $\mathbf{G}^{[2]}(\hat{\mathbf{x}}, \hat{t})$, can be expanded in Fourier series alongside the solution $\hat{v}^{[2]}$, i.e.

$$\hat{v}^{[2]}(\hat{\mathbf{x}}, \hat{t}) = \sum_{\nu \in \mathbb{Z}^2} \mathbf{c}_\nu^{[2]}(\hat{t}) e^{i\nu \cdot \hat{\mathbf{x}}}, \quad \mathbf{G}^{[2]}(\hat{\mathbf{x}}, \hat{t}) = \sum_{\nu \in \mathbb{Z}^2} \mathbf{g}_\nu^{[2]}(\hat{t}) e^{i\nu \cdot \hat{\mathbf{x}}}. \quad (86)$$

For the particular case of (84), the expansion consists of just a "reasonably small" number of non-vanishing harmonics but, more importantly, because of the dimension, the diagonalisation of the system (58), where

$$\Delta_\nu = \left(\frac{2\pi}{L} \right)^2 \begin{pmatrix} A_0\nu_1^2 + \Gamma_0\nu_2^2 & (B_0 + \Gamma_0)\nu_1\nu_2 \\ (B_0 + \Gamma_0)\nu_1\nu_2 & \Gamma_0\nu_1^2 + A_0\nu_2^2 \end{pmatrix},$$

relies on a particularly simple and exact expression for its eigenvalues

$$\lambda_{1,2} = (2\pi L^{-1})^2 (A_0 + \Gamma_0)(\nu_1^2 + \nu_2^2) \mp (2\pi L^{-1})^2 \sqrt{(A_0 - \Gamma_0)^2(\nu_1^2 - \nu_2^2)^2 + 4(B_0 + \Gamma_0)^2\nu_1^2\nu_2^2},$$

defining the diagonal matrix $\mathbf{\Lambda}$, while the matrix \mathbf{P} collects the eigenvectors and it is expressed in the form

$$\mathbf{P} = \begin{pmatrix} \lambda_1 - (2\pi L^{-1})^2 (\Gamma_0\nu_1^2 + A_0\nu_2^2) & \lambda_2 - (2\pi L^{-1})^2 (\Gamma_0\nu_1^2 + A_0\nu_2^2) \\ (2\pi L^{-1})^2 (B_0 + \Gamma_0)\nu_1\nu_2 & (2\pi L^{-1})^2 (B_0 + \Gamma_0)\nu_1\nu_2 \end{pmatrix}.$$

Remark 5.1. The determination of the Fourier coefficients appearing in (86) represents perhaps the main computational "challenge" of the whole scheme, being the mentioned coefficients depending on time.

5.3 Solutions from the asymptotic homogenization and spectro-hierarchical procedures

In order to compare the results obtained from the asymptotic homogenization procedure described in Section 3 with those derived from the spectro-hierarchical approach introduced in Section 4, we first consider zero initial conditions, as specified in equation (76). Assuming the reference stiffness and density to be $C_r = C_{1111}^{SiC}$ and $\rho_r = \rho^{SiC}$, respectively, the first column of Figure 3 illustrates the comparison among three solutions:

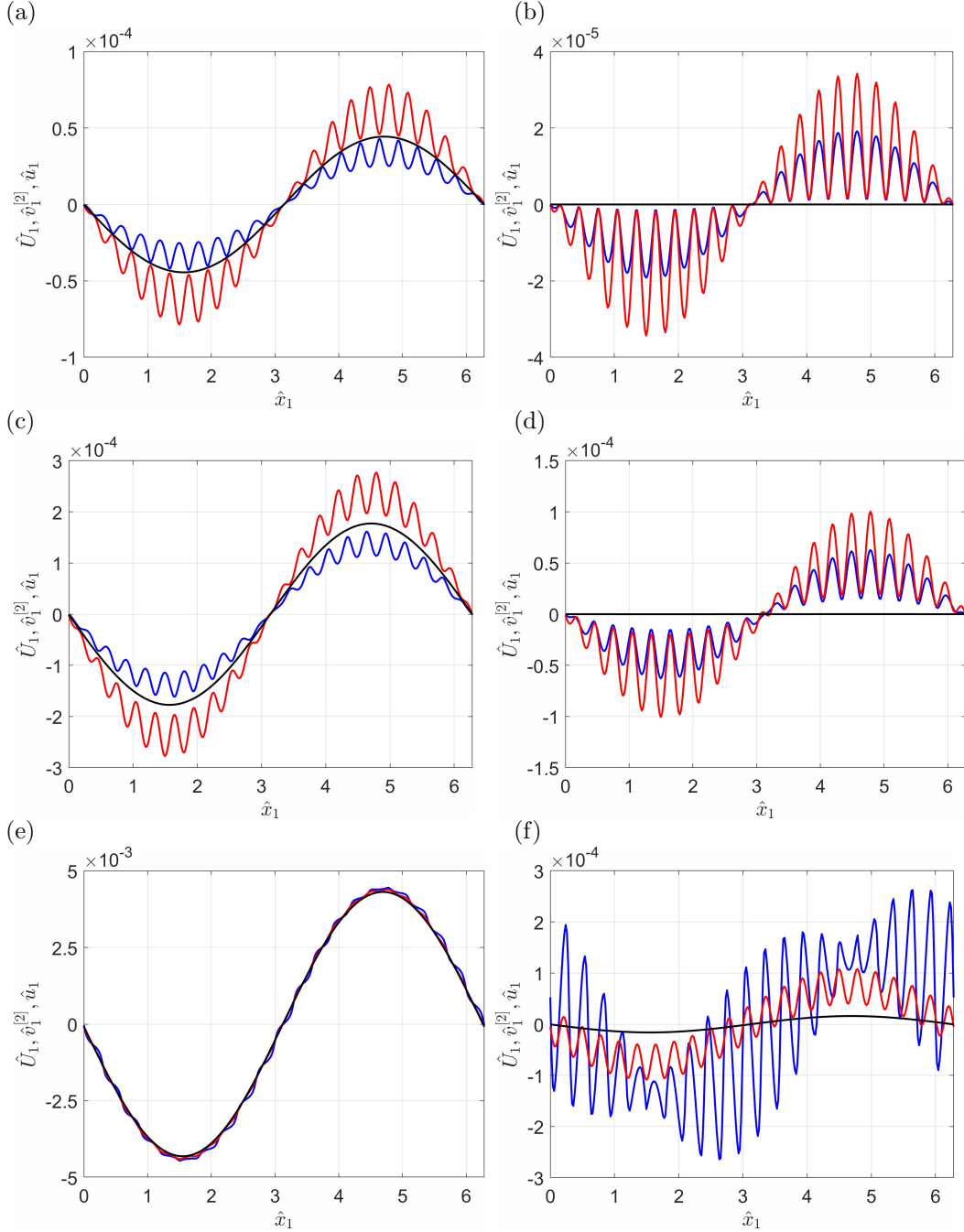


Figure 3: Zero initial conditions. Solutions \hat{U}_1 (black curves), $\hat{v}_1^{[2]}$ (red curves), and \hat{u}_1 (blue curves) vs \hat{x}_1 with $\hat{x}_2 = 0$ at $\hat{t}_1 = 1/100$ (a), $\hat{t}_1 = 1/50$ (c), and at $\hat{t}_1 = 1/10$ (e). Difference between solutions \hat{U}_1 , $\hat{v}_1^{[2]}$, \hat{u}_1 and $\hat{v}_1^{[1]}$ vs \hat{x}_1 with $\hat{x}_2 = 0$ at $\hat{t}_1 = 1/100$ (b), $\hat{t}_1 = 1/50$ (d), and at $\hat{t}_1 = 1/10$ (f).

the homogenized displacement field \hat{U}_1 (black curves), the second-order spectro-hierarchical solution $\hat{v}_1^{[2]}$ (red curves), and the heterogeneous reference solution \hat{u}_1 (blue curves). All quantities are plotted as functions of the normalized spatial coordinate \hat{x}_1 for $\hat{x}_2 = 0$, considering three distinct dimensionless time instants, namely $\hat{t}_1 = 1/100$, $\hat{t}_2 = 1/50$, and $\hat{t}_3 = 1/10$. The heterogeneous solution \hat{u}_1 has been obtained through a finite element simulation of a periodic cluster composed of 21 cells along the horizontal direction and a single cell along the vertical one. As previously detailed, this numerical setup ensures a sufficiently accurate representation of the microscale response. The second column of Figure 3 displays the differences between

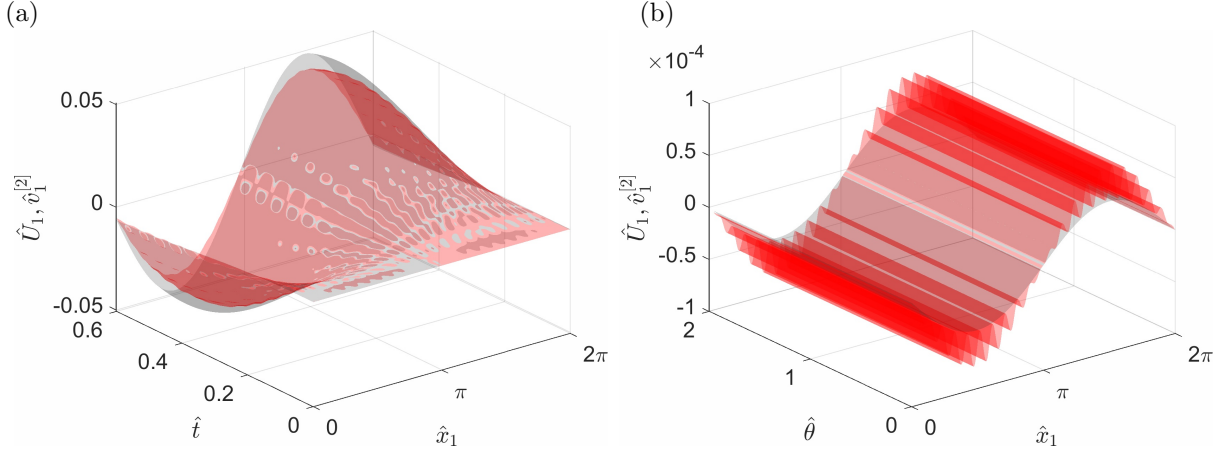


Figure 4: Zero initial conditions. Solutions \hat{U}_1 (black surface) and $\hat{v}_1^{[2]}$ (red surface) vs \hat{x}_1 and \hat{t} for $\hat{x}_2 = 0$ and $\hat{\theta} = 0.2$ (a). Solutions \hat{U}_1 (black surface) and $\hat{v}_1^{[2]}$ (red surface) vs \hat{x}_1 and $\hat{\theta}$ for $\hat{x}_2 = 0$ and $\hat{t} = 1/100$ (b).

the solutions $\hat{U}_1, \hat{v}_1^{[2]}$, and \hat{u}_1 with respect to $\hat{v}_1^{[1]}$, i.e., the first-order approximation provided by the spectro-hierarchical method, evaluated at the same three time instants. This representation highlights more clearly the improved accuracy of the second-order spectro-hierarchical solution $\hat{v}_1^{[2]}$, which successfully captures the oscillatory behavior and local fluctuations induced by the microstructural heterogeneity at all considered times. Figure 4-(a) further shows the evolution of the homogenized and spectro-hierarchical solutions, \hat{U}_1 and $\hat{v}_1^{[2]}$, as functions of \hat{x}_1 and \hat{t} , for a dimensionless frequency $\hat{\theta} = \theta L \sqrt{\rho_r / C_r} = 0.2$. In contrast, Figure 4(b) depicts the same solutions as functions of \hat{x}_1 and $\hat{\theta}$, evaluated at the first time instant $\hat{t} = \hat{t}_1$. When the initial conditions defined in equations (75) are instead considered, the results corresponding to the steady-state regime are presented in Figure 5. In particular, Figure 5(a) shows the displacement component along the direction \mathbf{e}_1 as a function of \hat{x}_1 for $\hat{x}_2 = 0$ at time instant \hat{t}_3 . The homogenized solution \hat{U}_1 (black curve) and the heterogeneous finite element solution \hat{u}_1 (blue curve) exhibit an excellent agreement, confirming the robustness of the homogenized model. The spectro-hierarchical steady-state solution $\hat{v}_1^{[2]}$ is represented by the red curve, while the corresponding heterogeneous reference response is plotted in magenta. Once again, the spectro-hierarchical formulation provides an accurate reproduction of the microscale behavior, capturing both the global and local features of the displacement field. For $\hat{x}_2 = 0$ and $\hat{\theta} = 0.2$, Figure 5(b) illustrates the time evolution of the displacement components \hat{U}_1 and $\hat{v}_1^{[2]}$ at $\hat{x}_1 = \pi$. Figures 5-(c) and 5-(d) display these quantities separately as functions of \hat{t} and \hat{x}_1 , highlighting the differences in temporal and spatial modulation. Finally, by fixing $\hat{x}_1 = \pi$, Figures 5-(e) and 5-(f) present the displacements \hat{U}_1 and $\hat{v}_1^{[2]}$ as functions of both \hat{t} and $\hat{\theta}$, providing a comprehensive picture of their dynamic and frequency-dependent behaviors.

6 Conclusions

The present study has systematically investigated the transient elastic response of two-dimensional periodic composites, with particular emphasis on capturing both macroscopic and microstructural dynamics. Solutions were obtained via the asymptotic homogenization approach, providing effective macroscopic equations that describe the overall behavior of the heterogeneous material and deliver a computationally efficient reduced-order model accurately reproducing long-wave and low-frequency responses. In parallel, a novel spectro-hierarchical procedure was employed, offering a robust hierarchical framework for resolving higher-order fluctuations and faithfully capturing fine-scale spatial and temporal features. By utilizing Fourier expansions, hierarchical truncations, and explicit treatment of transient effects, this method reconstructs both the first-order homogenized response and higher-order corrections due to microstructural variations, thus bridging the gap between homogenized and fully heterogeneous solutions.

The numerical investigations on the SiC-based microstructured composite demonstrate the clear advan-

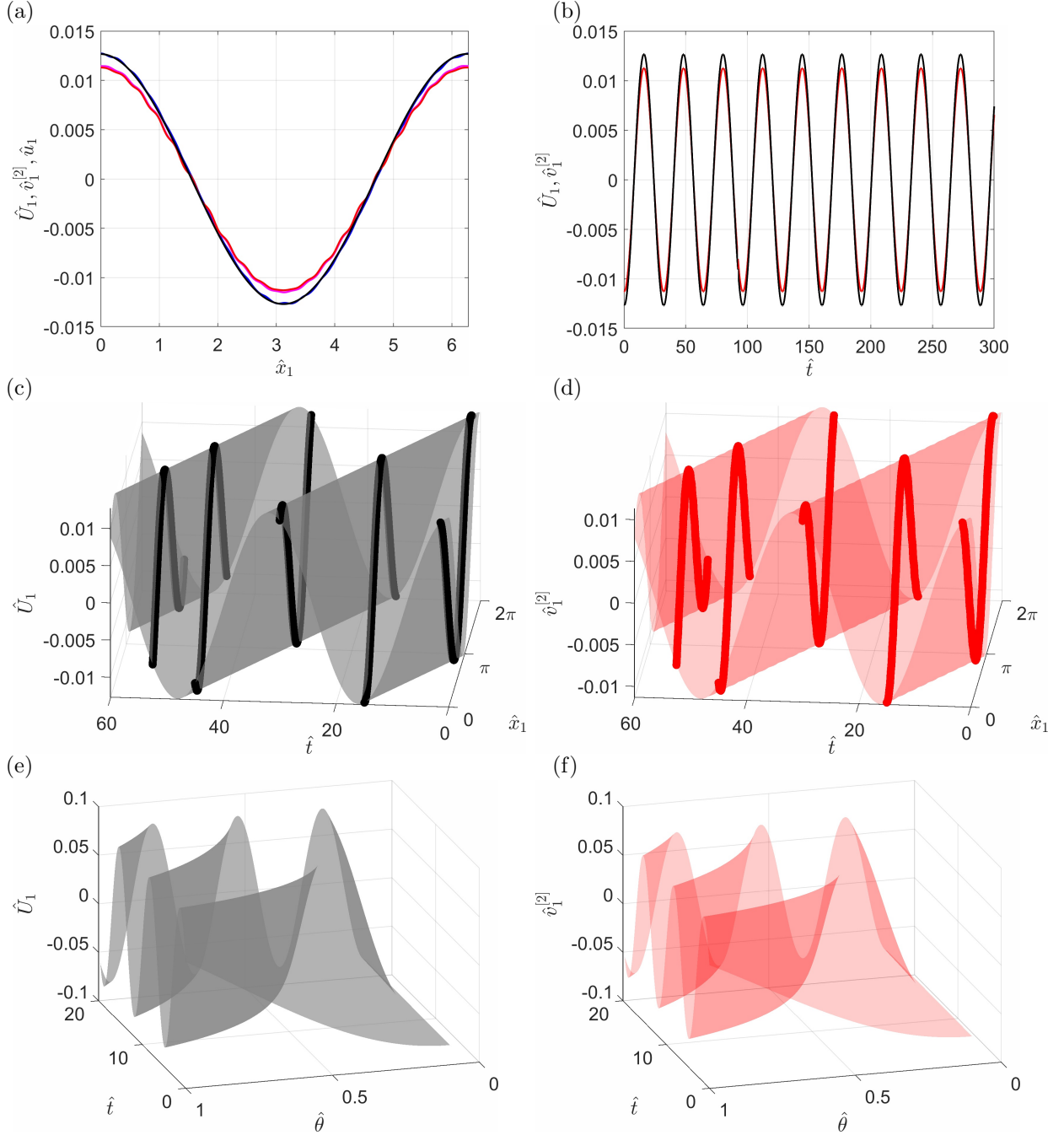


Figure 5: Steady-state solutions:(a) displacement \hat{U}_1 from asymptotic homogenization (black curve) and corresponding heterogeneous solution \hat{u}_1 (blue curve), and displacement $\hat{v}_1^{[2]}$ from spectro-hierarchical scheme (red curve) and corresponding heterogeneous solution \hat{u}_1 (magenta curve). Time instant equal to \hat{t}_3 ; (b) \hat{U}_1 (black) and $\hat{v}_1^{[2]}$ (red) vs \hat{t} at a point $(\hat{x}_1, \hat{x}_2) = (\pi, 0)$; (c) \hat{U}_1 as a function of \hat{x}_1 and \hat{t} at $\hat{\theta} = 0.2$; (d) $\hat{v}_1^{[2]}$ as a function of \hat{x}_1 and \hat{t} at $\hat{\theta} = 0.2$; (e) \hat{U}_1 as a function of \hat{t} and $\hat{\theta}$ at $\hat{x}_1 = \pi$; (f) $\hat{v}_1^{[2]}$ as a function of \hat{t} and $\hat{\theta}$ at $\hat{x}_1 = \pi$.

tage of the spectro-hierarchical method. For zero initial conditions, the second-order spectro-hierarchical solution precisely recovers microstructural fluctuations in the heterogeneous displacement field that are missed by the first-order homogenized solution, while maintaining excellent consistency with fully resolved numerical simulations. For non-zero initial conditions, the approach accurately captures the transient spa-

tiotemporal evolution of displacement components, effectively tracking elastic wave propagation through the microstructure and resolving frequency-dependent behaviors. These results underscore the method's robustness and its capacity to model short-time dynamics and high-frequency or localized excitations, providing insights that are difficult to obtain through standard homogenization techniques alone.

Overall, this work establishes the combined use of asymptotic homogenization and the spectro-hierarchical framework as a versatile and comprehensive toolkit for the transient analysis of periodic composites. While the homogenization method provides computationally efficient macroscopic predictions, the procedure denoted as spectro-hierarchical resolves fine-scale dynamics and higher-order effects, effectively bridging the gap between reduced-order and fully heterogeneous models. The study highlights the added value of explicitly considering transient dynamics and microstructural corrections. Future research will focus on extending the spectro-hierarchical methodology to three-dimensional microstructures, incorporating viscoelastic and thermo-mechanical couplings, and addressing microscale nonlinearities. These advancements are expected to broaden the applicability of the proposed approach to cutting-edge engineering materials and functional composites, where transient, frequency-dependent, and localized behaviors critically influence the performance, reliability, and design optimization.

Acknowledgments

F. Fantoni, A. Bacigalupo are members of INdAM-GNFM. The authors gratefully acknowledge the National Group of Mathematical Physics (GNFM-INdAM, Italy), the financial support of the European Union – Next Generation EU, under the call PRIN 2022 of the Italian Minister of University and Research (MUR) - Project 202222LB37 (PE: Physical Sciences and Engineering): “Advanced Design of avant-garde ACTIVE microstructured materials via additive manufacturing (ADACTIVE)”.

Appendix A: Solution of recursive differential problems

Asymptotic expansion (12) of the micro field equation in powers of the parameter ε leads to a series of recursive differential problems in terms of sensitivities $\bar{u}_i^{(j)}$, with $j = 0, 1, 2, \dots$. At the order ε^{-2} , the resulting partial differential equation and relative initial condition take the form

$$\begin{cases} \left(\bar{C}_{ijhk}^m \bar{u}_{h,k}^{(0)} \right)_{,j} = f_i^{(0)}(\bar{\mathbf{x}}, \bar{t}), \\ \bar{u}_i^{(0)}(\bar{\mathbf{x}}, \bar{\boldsymbol{\xi}}, \bar{t} = 0) = \bar{v}_{0_i}(\bar{\mathbf{x}}), \\ \frac{\partial \bar{u}_i^{(0)}}{\partial \bar{t}}(\bar{\mathbf{x}}, \bar{\boldsymbol{\xi}}, \bar{t} = 0) = \bar{w}_{0_i}(\bar{\mathbf{x}}) \end{cases} \quad (87)$$

The problem (87) is equipped with interface conditions

$$\left[\left[\bar{u}_i^{(0)} \right] \right] \Big|_{\bar{\boldsymbol{\xi}} \in \Sigma_1} = 0, \quad \left[\left[\bar{C}_{ijhk}^m \bar{u}_{h,k}^{(0)} n_j \right] \right] \Big|_{\bar{\boldsymbol{\xi}} \in \Sigma_1} = 0. \quad (88)$$

The solvability condition for problem (87) in the class of \bar{Q} -periodic functions involves that $f_i^{(0)} = 0$ (see [42]) and, in view of this, the sensitivity $\bar{u}_i^{(0)}$ results to be $\bar{\boldsymbol{\xi}}$ -independent and assumes the form

$$\bar{u}_i^{(0)} = \bar{U}_i(\bar{\mathbf{x}}, \bar{t}). \quad (89)$$

Taking into account the solution (89) of the problem at the order ε^{-2} , the micro recursive differential problem at the order ε^{-1} results

$$\begin{cases} \left(\bar{C}_{ijhk}^m \bar{u}_{h,k}^{(1)} \right)_{,j} + \bar{C}_{ijhk}^m \frac{\partial \bar{U}_h}{\partial \bar{x}_k} = f_i^{(1)}(\bar{\mathbf{x}}, \bar{t}), \\ \bar{u}_i^{(1)}(\bar{\mathbf{x}}, \bar{\boldsymbol{\xi}}, \bar{t} = 0) = 0, \\ \frac{\partial \bar{u}_i^{(1)}}{\partial \bar{t}}(\bar{\mathbf{x}}, \bar{\boldsymbol{\xi}}, \bar{t} = 0) = 0. \end{cases} \quad (90)$$

Its interface conditions read

$$\left[\left[\bar{u}_i^{(1)} \right] \right] \Big|_{\bar{\boldsymbol{\xi}} \in \Sigma_1} = 0, \quad \left[\left[\bar{C}_{ijhk}^m \left(\frac{\partial \bar{U}_h}{\partial \bar{x}_k} + \bar{u}_{h,k}^{(1)} \right) n_j \right] \right] \Big|_{\bar{\boldsymbol{\xi}} \in \Sigma_1} = 0. \quad (91)$$

Denoting again with $\langle \cdot \rangle = \frac{1}{|\bar{\mathcal{Q}}|} \int_{\bar{\mathcal{Q}}} (\cdot) d\bar{\xi}$, because of solvability condition of problem (90), the source term reads

$$f_i^{(1)}(\bar{\mathbf{x}}, \bar{t}) = \langle \bar{C}_{ijhk}^m \rangle \frac{\partial \bar{U}_h}{\partial \bar{x}_k}, \quad (92)$$

where the $\bar{\mathcal{Q}}$ -periodicity of micro elasticity tensor and the divergence theorem entail that $f_i^{(1)}(\bar{\mathbf{x}}, \bar{t}) = 0$. Solution of problem at the order ε^{-1} , therefore, assumes the form

$$\bar{u}_i^{(1)}(\bar{\mathbf{x}}, \bar{\xi}, \bar{t}) = \bar{N}_{ipq_1}^{(1)}(\bar{\xi}, \bar{t}) \frac{\partial \bar{U}_p(\bar{\mathbf{x}}, \bar{t})}{\partial \bar{x}_{q_1}}. \quad (93)$$

The solution (89) of problem at the order ε^{-2} and the solution (93) of problem at the order ε^{-1} lead to express the micro differential problem at the order ε^0 in the following form, symmetrized with respect to indexes q_1 and q_2

$$\begin{cases} \left(\bar{C}_{ijhk}^m \bar{u}_{h,k}^{(2)} \right)_{,j} + \frac{1}{2} \left[\left(\bar{C}_{ijhq_2}^m \bar{N}_{hpq_1}^{(1)} \right)_{,j} + \bar{C}_{iq_1pq_2}^m + \bar{C}_{iq_2hj}^m \bar{N}_{hpq_1,j}^{(1)} + \right. \\ \left. + \left(\bar{C}_{ijhq_1}^m \bar{N}_{hpq_2}^{(1)} \right)_{,j} + \bar{C}_{iq_2pq_1}^m + \bar{C}_{iq_1hj}^m \bar{N}_{hpq_2,j}^{(1)} \right] \frac{\partial^2 \bar{U}_p}{\partial \bar{x}_{q_1} \partial \bar{x}_{q_2}} - \bar{\rho}^m \frac{\partial^2 \bar{U}_i}{\partial \bar{t}^2} = f_i^{(2)}(\bar{\mathbf{x}}, \bar{t}), \\ \bar{u}_i^{(2)}(\bar{\mathbf{x}}, \bar{\xi}, \bar{t} = 0) = 0, \\ \frac{\partial \bar{u}_i^{(2)}}{\partial \bar{t}}(\bar{\mathbf{x}}, \bar{\xi}, \bar{t} = 0) = 0. \end{cases} \quad (94)$$

Interface conditions for problem (94) read

$$\left[\left[\bar{u}_i^{(2)} \right] \right] \Big|_{\bar{\xi} \in \Sigma_1} = 0, \quad \left[\left[\bar{C}_{ijhk}^m \left(\bar{N}_{hpq_1}^{(1)} \frac{\partial^2 \bar{U}_p}{\partial \bar{x}_{q_1} \partial \bar{x}_k} + \bar{u}_{h,k}^{(2)} \right) n_j \right] \right] \Big|_{\bar{\xi} \in \Sigma_1} = 0. \quad (95)$$

The solvability condition for problem (94) guarantees that

$$f_i^{(2)}(\bar{\mathbf{x}}, \bar{t}) = \frac{1}{2} \left\langle \bar{C}_{iq_2hj}^m \bar{N}_{hpq_1,j}^{(1)} + \bar{C}_{iq_1pq_2}^m + \bar{C}_{iq_1hj}^m \bar{N}_{hpq_2,j}^{(1)} + \bar{C}_{iq_2pq_1}^m \right\rangle \frac{\partial^2 \bar{U}_p}{\partial \bar{x}_{q_1} \partial \bar{x}_{q_2}} - \langle \bar{\rho}^m \rangle \frac{\partial^2 \bar{U}_i}{\partial \bar{t}^2}, \quad (96)$$

from which the solution $\bar{u}_i^{(2)}$ at the order ε^0 reads

$$\bar{u}_i^{(2)}(\bar{\mathbf{x}}, \bar{\xi}, \bar{t}) = \bar{N}_{ipq_1q_2}^{(2)}(\bar{\xi}, \bar{t}) \frac{\partial^2 \bar{U}_p(\bar{\mathbf{x}}, \bar{t})}{\partial \bar{x}_{q_1} \partial \bar{x}_{q_2}} + \bar{N}_{ip}^{(2,2)}(\bar{\xi}, \bar{t}) \frac{\partial^2 \bar{U}_p(\bar{\mathbf{x}}, \bar{t})}{\partial \bar{t}^2}. \quad (97)$$

The solution of higher-order microscopic differential problems can be obtained following the procedure detailed in the present Appendix without introducing further difficulties.

References

- [1] M. Khalid, Z. Arif, A. Tariq, M. Hossain, R. Umer, and M. Bodaghi. 3d printing of active mechanical metamaterials: A critical review. *Materials & Design*, 246:113305, 2024.
- [2] S. Yuan, C. Chua, and K. Zhou. 3d-printed mechanical metamaterials with high energy absorption. *Advanced Materials Technologies*, 4(3):1800419, 2019.
- [3] A. Nazir, O. Gokcekaya, K. Billah, O. Ertugrul, J. Jiang, J. Sun, and S. Hussain. Multi-material additive manufacturing: A systematic review of design, properties, applications, challenges, and 3d printing of materials and cellular metamaterials. *Materials & Design*, 226:111661, 2023.
- [4] H. Cui, D. Yao, R. Hensleigh, H. Lu, A. Calderon, Z. Xu, S. Davaria, Z. Wang, P. Mercier, P. Tarazaga, et al. Design and printing of proprioceptive three-dimensional architected robotic metamaterials. *Science*, 376(6599):1287–1293, 2022.

- [5] D. Misseroni, P. Pratapa, K. Liu, and G. Paulino. Experimental realization of tunable poisson’s ratio in deployable origami metamaterials. *Extreme Mechanics Letters*, 53:101685, 2022.
- [6] M. Geers, V. Kouznetsova, and W. Brekelmans. Computational homogenization. In *Multiscale modelling of plasticity and fracture by means of dislocation mechanics*, pages 327–394. Springer, 2010.
- [7] N. Charalambakis. Homogenization techniques and micromechanics. a survey and perspectives. *Applied Mechanics Reviews*, 63(3), 2010.
- [8] N. Bakhvalov and G. Panasenko. *Homogenization: Averaging Processes in Periodic Media*. Kluwer Academic Publishers, Dordrecht-Boston-London, 1984.
- [9] A. Bensoussan, J.-L. Lions, and G. Papanicolaou. *Asymptotic analysis for periodic structures*. North-Holland, Amsterdam, 1978.
- [10] I. Kamotski and V. Smyshlyaev. Bandgaps in two-dimensional high-contrast periodic elastic beam lattice materials. *Journal of the Mechanics and Physics of Solids*, 123:292–304, 2019.
- [11] L. Molotkov. On methods of deriving equations describing effective models of layered media. *Journal of Mathematical Sciences*, 102:4275–4290, 2000.
- [12] V. Smyshlyaev and K. Cherednichenko. On rigorous derivation of strain gradient effects in the overall behaviour of periodic heterogeneous media. *Journal of the Mechanics and Physics of Solids*, 48(6):1325–1357, 2000.
- [13] I. Andrianov, A. Kolpakov, and L. Faella. Asymptotic model of a piezoelectric composite beam. *Journal of Applied Mechanics and Technical Physics*, 65(2):345–353, 2024.
- [14] X. Chen, J. Yvonnet, S. Yao, and H. Park. Topology optimization of flexoelectric composites using computational homogenization. *Computer Methods in Applied Mechanics and Engineering*, 381:113819, 2021.
- [15] F. Fantoni, A. Bacigalupo, and M. Paggi. Multi-field asymptotic homogenization of thermo-piezoelectric materials with periodic microstructure. *International Journal of Solids and Structures*, 120:31–56, 2017.
- [16] F. Fantoni, A. Bacigalupo, and M. Paggi. Design of thermo-piezoelectric microstructured bending actuators via multi-field asymptotic homogenization. *International Journal of Mechanical Sciences*, 146:319–336, 2018.
- [17] A. Bacigalupo, L. Morini, and A. Piccolroaz. Multiscale asymptotic homogenization analysis of thermo-diffusive composite materials. *International Journal of Solids and Structures*, 85:15–33, 2016.
- [18] F. Fantoni and A. Bacigalupo. Wave propagation modeling in periodic elasto-thermo-diffusive materials via multifield asymptotic homogenization. *International Journal of Solids and Structures*, 196:99–128, 2020.
- [19] A. Salvadori, E. Bosco, and D. Grazioli. A computational homogenization approach for li-ion battery cells: Part 1 – formulation. *Journal of the Mechanics and Physics of Solids*, 65:114–137, 2014.
- [20] R. Bengtsson, M. Mousavi, R. Afshar, and E. Gamstedt. Viscoelastic behavior of softwood based on a multiscale computational homogenization. *Mechanics of materials*, 179:104586, 2023.
- [21] R. Del Toro, A. Bacigalupo, and M. Paggi. Characterization of wave propagation in periodic viscoelastic materials via asymptotic-variational homogenization. *International Journal of Solids and Structures*, 172:110–146, 2019.
- [22] L. Ferreira, P. Lopes, R. Leiderman, F.T.S. Aragão, and A.M.B. Pereira. An image-based numerical homogenization strategy for the characterization of viscoelastic composites. *International Journal of Solids and Structures*, 267:112142, 2023.

- [23] R. Del Toro, F. Fantoni, M. De Bellis, and A. Bacigalupo. A multiscale approach to visco-electro-elastic complex materials: Asymptotic homogenization versus high-frequency continualization schemes. *International Journal of Engineering Science*, 216:104331, 2025.
- [24] Q. Yu and J. Fish. Multiscale asymptotic homogenization for multiphysics problems with multiple spatial and temporal scales: a coupled thermo-viscoelastic example problem. *International journal of solids and structures*, 39(26):6429–6452, 2002.
- [25] E. Bosco, R. Claessens, and A. Suiker. Multi-scale prediction of chemo-mechanical properties of concrete materials through asymptotic homogenization. *Cement and Concrete Research*, 128:105929, 2020.
- [26] B. Pal and A. Ramaswamy. A multi-physics-based approach to predict mechanical behavior of concrete element in a multi-scale framework. *Mechanics of Materials*, 176:104509, 2023.
- [27] C. Vega, J. Pina, E. Bosco, E. Flores, C. Guzman, and S. Yanez. Thermo-mechanical analysis of wood through an asymptotic homogenisation approach. *Construction and Building Materials*, 315:125617, 2022.
- [28] L. Miller and R. Penta. Effective balance equations for poroelastic composites. *Continuum Mechanics and Thermodynamics*, 32(6):1533–1557, 2020.
- [29] L. Miller and R. Penta. Homogenized multiscale modelling of an electrically active double poroelastic material representing the myocardium. *Biomechanics and Modeling in Mechanobiology*, 24(2):635–662, 2025.
- [30] D. Prève, A. Bacigalupo, and M. Paggi. Variational-asymptotic homogenization of thermoelastic periodic materials with thermal relaxation. *International Journal of Mechanical Sciences*, page 106566, 2021.
- [31] E. Rudoy and S. Sazhenkov. The homogenized dynamical model of a thermoelastic composite stitched with reinforcing filaments. *Philosophical Transactions A*, 382(2277):20230304, 2024.
- [32] H. Zhang, S. Zhang, J. Bi, and B. Schrefler. Thermo-mechanical analysis of periodic multiphase materials by a multiscale asymptotic homogenization approach. *International Journal for Numerical Methods in Engineering*, 69(1):87–113, 2007.
- [33] I. Temizer. On the asymptotic expansion treatment of two-scale finite thermoelasticity. *International Journal of Engineering Science*, 53:74–84, 2012.
- [34] C. Böhm, B. Hudobivnik, M. Marino, and P. Wriggers. Electro-magneto-mechanically response of polycrystalline materials: Computational homogenization via the virtual element method. *Computer Methods in Applied Mechanics and Engineering*, 380:113775, 2021.
- [35] L. Borcea and O. Bruno. On the magneto-elastic properties of elastomer–ferromagnet composites. *Journal of the Mechanics and Physics of Solids*, 49(12):2877–2919, 2001.
- [36] I. Christofi, D. Hadjiloizi, A. Kalamkarov, and A. Georgiades. Dynamic micromechanical model for smart composite and reinforced shells. *ZAMM-Journal of Applied Mathematics and Mechanics/Zeitschrift für Angewandte Mathematik und Mechanik*, 102(5):e202100211, 2022.
- [37] A. Fortunati. Travelling waves over an arbitrary bathymetry: a local stability result. *Dyn. Partial Differ. Equ.*, 15(1):81–94, 2018.
- [38] A. Giorgilli. Exponential stability of Hamiltonian systems. In *Dynamical systems. Part I*, Pubbl. Cent. Ric. Mat. Ennio Giorgi, pages 87–198. Scuola Norm. Sup., Pisa, 2003.
- [39] A. Fortunati and S. Wiggins. Normal form and Nekhoroshev stability for nearly integrable Hamiltonian systems with unconditionally slow aperiodic time dependence. *Regul. Chaotic Dyn.*, 19(3):363–373, 2014.

- [40] A. Fortunati and S. Wiggins. Negligibility of small divisor effects in the normal form theory for nearly-integrable Hamiltonians with decaying non-autonomous perturbations. *Celest. Mech. Dyn. Astr.*, 125:247–262, 2016.
- [41] V. Smyshlyaev and K. Cherednichenko. On rigorous derivation of strain gradient effects in the overall behaviour of periodic heterogeneous media. *J. Mech. Phys. Solids*, 48:1325–1357, 2000.
- [42] N. Bakhvalov and G. Panasenko. *Homogenization: averaging processes in periodic media*. Kluwer Academic Publishers, Dordrecht-Boston-London, 1984.
- [43] A. Bacigalupo. Second-order homogenization of periodic materials based on asymptotic approximation of the strain energy: formulation and validity limits. *Meccanica*, 49:1407–1425, 2014.
- [44] R. Paley and N. Wiener. *Fourier transforms in the complex domain*, volume 19. American Mathematical Soc., 1934.
- [45] A. Bacigalupo and L. Gambarotta. Second-gradient homogenized model for wave propagation in heterogeneous periodic media. *Int. J. Solids Struct.*, 51:1052–1065, 2014.
- [46] M. De Bellis, A. Bacigalupo, and G. Zavarise. Characterization of hybrid piezoelectric nanogenerators through asymptotic homogenization. *Computer Methods in Applied Mechanics and Engineering*, 355:1148–1186, 2019.
- [47] F. Fantoni and A. Bacigalupo. Multifield constitutive identification of non-conventional thermo-viscoelastic periodic cauchy materials. *International Journal of Mechanical Sciences*, 223:107228, 2022.
- [48] N. Nekhoroshev. An exponential estimate on the time of stability of nearly-integrable Hamiltonian systems. *Russ. Math. Surveys*, 32:1–65, 1977.
- [49] N. Nekhoroshev. An exponential estimate on the time of stability of nearly-integrable Hamiltonian systems II. *Trudy Sem. Petrovs.*, 5:5–50, 1979.
- [50] A. Giorgilli and L. Galgani. Rigorous estimates for the series expansions of Hamiltonian perturbation theory. *Celestial Mech.*, 37(2):95–112, 1985.